ORNL/TM-7481

ornl

OAK RIDGE NATIONAL LABORATORY

UNION CARBIDE

Analysis of Heat Transfer in Building Thermal Insulation

H. A. Fine
S. H. Jury
D. W. Yarbrough
D. L. McElroy

Part of
The National Program
for
Building Thermal Envelope Systems and Insulating Materials

PREPARED FOR THE DEPARTMENT OF ENERGY
CONSERVATION AND SOLAR ENERGY
OFFICE OF BUILDINGS AND COMMUNITY SYSTEMS
BUILDINGS DIVISION

OPERATED BY
UNION CARBIDE CORPORATION
FOR THE UNITED STATES
DEPARTMENT OF ENERGY

DISCLAIMER

Printed in the United States of America. Available from
National Technical Information Service
U.S. Department of Commerce
5285 Port Royal Road, Springfield, Virginia 22161
NTIS price codes—Printed Copy: A05 Microfiche A01

MASTER

ORNL/TM-7481
Distribution
Category UC-95d

Contract No. W-7405-eng-26

ANALYSIS OF HEAT TRANSFER IN BUILDING THERMAL INSULATION

H. A. Fine
Department of Metallurgical Engineering and Materials Science
University of Kentucky
Lexington, KY 40506

S. H. Jury
Department of Chemical Engineering (Retired)
University of Tennessee
Knoxville, TN 37916

D. W. Yarbrough and D. L. McElroy
Metals and Ceramics Division
Oak Ridge National Laboratory
Oak Ridge, TN 37830

Part of
The National Program
for
Building Thermal Envelope Systems and Insulating Materials
Research Sponsored by the
Office of Buildings and Community Systems

Date Published: December 1980

NOTICE: This document contains information of preliminary nature. It is subject to revision or correction and therefore does not represent a final report.

OAK RIDGE NATIONAL LABORATORY
Oak Ridge, Tennessee 37830
operated by
UNION CARBIDE CORPORATION
for the
DEPARTMENT OF ENERGY

feq

THIS PAGE

WAS INTENTIONALLY

LEFT BLANK

CONTENT

THIS PAGE

WAS INTENTIONALLY

LEFT BLANK

FOREWORD

This is one of a series of reports describing research, development, and demonstration activities in support of the National Program for Building Thermal Envelope Systems and Insulating Materials. The national program involves several federal agencies and many other organizations in the public and private sectors that are addressing the national objective of decreasing energy waste in the heating and cooling of buildings. Results described in this report are part of the national program through delegation of management responsibilities for the DOE lead role to Oak Ridge National Laboratory.

Other reports in this series include the following, which are available from NTIS:

1. DOE/CS-0059, *The National Program Plan for Building Thermal Envelope Systems and Insulating Materials* (January 1979);
2. ORNL/SUB-7556/1, *Assessment of the Corrosiveness of Cellulosic Insulating Materials* (June 1979).
3. ORNL/SUB-7504/3, *Recessed Light Fixture Test Facility* (July 1979).
4. ORNL/SUB-7559/1, *Problems Associated with the Use of Urea-Formaldehyde Foam for Residential Insulation* (September 1979).
5. ORNL/SUB-7551/1, *Interim Progress Report on an Investigation of Energy Transport in Porous Insulator Systems* (October 1979).
6. ORNL/TM-6494, *A Technique for Measuring the Apparent Conductivity of Flat Insulations* (October 1979).
7. ORNL/SUB-79/13660/1, *Minnesota Retrofit Insulation In Situ Test Program Extension and Review* (February 1980).
8. ORNL/TM-7266, *An Experimental Study of Thermal Resistance Values (R-Values) of Low-Density Mineral-Fiber Building Insulation Batts Commercially Available in 1977* (April 1980).

Ted S. Lundy
Program Manager
Building Thermal Envelope Systems
and Insulating Materials
Oak Ridge National Laboratory

E. C. Freeman
Program Manager, Buildings Divison
Office of Building and Community Systems
Department of Energy

THIS PAGE

WAS INTENTIONALLY

LEFT BLANK

EDITOR'S NOTE

Although ORNL has a policy of reporting its work in SI metric units, this report uses English units. The justification is that the insulation industry at present operates completely with English units, and reporting otherwise would lose meaning to the intended readership. To assist the reader in obtaining the SI equivalents, these are listed below for the units occurring in this report.

Property	Unit Used	SI Equivalent
Dimension	in.	25.4 mm
Dimension	ft	0.3048 m
Density	lb/ft^3	16.02 kg/m^3
Power	Btu/h	0.2929 W
Thermal conductivity	Btu in./h ft^2 °F	0.1441 W/m K
Thermal resistance	h ft^2 °F/Btu	0.1762 K m^2/W
Temperature	°F	°C = (5/9)(°F − 32)
Temperature difference	°F	°C = (5/9)°F

ACKNOWLEDGMENTS

The authors wish to thank J. P. Moore of the Metals and Ceramics Division for reviewing the draft report and T. G. Godfrey, Metals and Ceramics Division, for his review of the draft report and help in developing the PDP/8e computer program. We also acknowledge F. J. Weaver and R. S. Graves for help in data processing. We also wish to thank Sharon Buhl and Jane Anderson for careful typing of several drafts, M. R. Sheldon for her technical editing efforts, and the Reports Office staff for preparation of the final report.

ANALYSIS OF HEAT TRANSFER IN BUILDING THERMAL INSULATION

H. A. Fine, S. H. Jury, D. W. Yarbrough, and D. L. McElroy

ABSTRACT

The measurement of the apparent thermal properties (i.e., conductivity, resistivity, and resistance) of insulation by the guarded hot-plate technique is mathematically simulated on a computer by assuming that coupled conductive and radiative heat transfer occurs in an absorbing and emitting single-phase gray medium. Calculations are performed for insulation extinction coefficients between 0.001 and 1000 ft^{-1}, thicknesses between 0.0208 and 1.0 ft, continuous-phase thermal conductivities between 0.1800 and 0.1980 Btu in./(h ft^2 °F), hot-plate temperatures between 485 and 635°R, and cold-plate temperatures between 435 and 585°R.

A three-region approximate solution to coupled conductive and radiative heat transfer in an infinite slab of absorbing and emitting gray material bounded by black surfaces is also developed and shown to agree to within ±0.5% of the numerical results for most cases. The approximate solution to the coupled problem and the exact solution to the uncoupled problem are used to establish the effect of test conditions (such as specimen thickness, plate emissivity, plate temperatures, and continuous-phase thermal conductivity) on the measured apparent thermal properties of an insulation specimen.

Examples of the temperature profiles within the insulation and a table of representative thicknesses for guarded hot-plate test specimens (i.e., the minimum specimen thickness required for measurement of an apparent thermal resistivity that is within 2% of the value at infinite thickness) are also presented.

A means to extrapolate thermal resistance data from thin to thick specimens is suggested by this analysis. Predictions from the extrapolation are shown to be consistent with existing thermal resistance data on low-density mineral fiber building insulation batts.

---

1. INTRODUCTION

Heat transfer within insulation may occur by conduction and radiation in the solid phase and by conduction, convection, and radiation in the gas phase. These mechanisms interact and combine to produce the total heat flux through the insulation and the temperature profile within the

insulation. The primary goal of this study is to understand how conduction and radiation interact to yield the thermal properties of insulation without the influence of convection.*

In general, a useful understanding of a complicated heat transfer problem is sought from analysis of experimental data using theoretical models of the interacting phenomena. Although several theoretical models exist,[1,2] virtually no experimental data can be found in the literature for the problem of interest. Several significant events have occurred since 1976 that have focused attention on the need for additional theoretical and experimental analyses of heat transfer in insulation. These events are outlined below. A new theoretical approach that clearly shows the relationship between two modes of heat transfer within insulation and the properties of the insulation and test facility follows.

First, in 1976, the American Society for Testing and Materials (ASTM) approved a significant change in the ASTM C177 specification for the standard guarded hot-plate test method.[3] Among the changes, ASTM C177-76 provided a new method to estimate the maximum thickness of specimens that can be used in the guarded hot-plate apparatus; the specification also noted that the thermal properties of a specimen may change with specimen thickness. Prior to this change, the maximum thickness was limited to one-third of the lateral dimension of the central section of the apparatus. Since the lateral dimensions of most central sections were less than 6 in., the majority of tests were conducted at a specimen thickness of less than 2 in. Thus prior to 1976, few studies provided data sets on the specimen thickness effect, and a linear extrapolation of any available data to design thickness was employed. The C177-76 specification, however, indicated the need for measurements on insulations at their design or full or actual-use thickness.

Second, since 1976, a number of laboratories have increased the central section dimension to 12 in., which by the pre-1976 specification would allow sample thicknesses up to 4 in. but by the new specification

*In this analysis convection is estimated as enhanced conduction (Sect. 2.7).

allow thicknesses of 6 in. or more. These devices should provide direct experimental data on the effect of thickness, assuming that the increased thickness does not increase the measurement error.

Although ASTM has endorsed the philosophy of full-thickness testing, a cautionary statement has been appended to C177-76 and a position statement prepared.[4] Both suggest that identification of measurement accuracy and the full-thickness effect require calibration standards, which do not exist.

Third, in 1979, the Federal Trade Commission (FTC) issued a final rule on labeling and advertising of home insulation that includes prescribed standardized test methods for determining *R*-values of home insulation materials.[5] The rule states all tests must be performed at a specimen thickness greater than that for which the apparent thermal resistivity of the material does not change by more than 2% with further increases in thickness. The effective date of this rule was to have been November 30, 1979, but this has been delayed.

Later in 1979, the Department of Energy (DOE) Residential Conservation Service (RCS) program issued a final rule,[6] which became effective December 7, 1979, and would recognize the FTC final rule as including requirements for thermal resistance testing. Since the RCS program is a major federal effort to encourage energy conservation measures, such as application of home insulation, the understanding of full-thickness testing is an important part of the national effort for energy conservation.

For an infinite planar section of insulation at steady state, the total heat flux is a constant that is independent of position within the specimen. Thus, the thermal conductivity, resistivity, and resistance to heat transfer of an insulating material may be defined by analogy to pure conductive heat transfer. (See Appendix A1 for the definitions given in ASTM C177-76.) However, while the total heat flux must be constant, the fraction of energy carried by each mechanism varies, with a nonlinear temperature profile resulting even when the properties are not a function of temperature. Because of the presence of radiative heat transfer, the thermal properties of insulation are apparent thermal properties that are a function of the physical and optical properties of the insulation and its bounding surfaces.

Realizing that measured values for the thermal properties of insulation may depend on the apparatus as well as the insulation, several investigators have employed limiting-case solutions to the actual heat transfer problem to define the effect of measurement conditions on the measured result.[7-9] These attempts have generally been based either on uncoupled (i.e., noninteracting) conductive, and radiative heat transfer in an absorbing, emitting, and scattering single-phase gray medium[7,8] or on conductive plus radiative heat transfer with only scattering.[9]

Exact solutions to the coupled conductive and radiative heat transfer problem for absorbing, emitting, and isotropically scattering single-phase gray materials bounded by nonblack isothermal infinite parallel plates have been developed by Viskanta[1] and by Lii and Ozisik.[2] These analyses show that a linear temperature profile exists only for the pure scattering case and that as the importance of scattering relative to absorption decreases the nonlinearity of the temperature profile increases. The worst limiting case, as indicated by the most nonlinear temperature profile, occurs for black bounding surfaces and no scattering within the material.

In the current work, the measurement of the apparent thermal properties (i.e., conductivity, resistivity, and resistance) of insulation by the guarded hot-plate technique is modeled using a digital computer that solves the coupled conductive and radiative heat transfer problem for an absorbing and emitting single-phase gray medium bounded by infinite parallel black isothermal plates. The results of these calculations for the worst limiting case and the previously determined results for the best limiting case are used to bracket the effect of sample thickness on the apparent thermal properties of insulation and to develop an extrapolation equation that shows the relationship between the apparent thermal properties and the measurement conditions (e.g., hot- and cold-plate emissivities and temperatures and specimen thickness).

2. THEORETICAL CONSIDERATIONS

In a properly designed and operated guarded hot plate, the guards minimize lateral heat exchange with the metered section so that a net flux occurs only in the direction normal to the hot and cold specimen surfaces.

Under these conditions, the specimen is equivalent to an infinite slab of the same thickness. The heat flux and temperature profile within the slab and the specimen are identical. Thus, heat transfer by coupled conduction and radiation in an absorbing and emitting single-phase gray slab bounded by infinite, black, isothermal, parallel plates approximates the worst limiting case for heat transfer within an insulation sample contained in a guarded hot plate with the hot plate up.

2.1 The Viskanta and Grosh Analysis

The temperature profile and total heat flux for the general coupled radiation and conduction problem are functions of the emissivities of the bounding surfaces and four dimensionless parameters that describe the sample and test conditions:

$$\theta_2 = \frac{\text{cold surface absolute temperature}}{\text{hot surface absolute temperature}} = \frac{T_2}{T_1} \text{ (reduced temperature)} , \tag{1}$$

$$\tau^\circ = \frac{L}{1/E} = \frac{\text{sample thickness}}{\text{photon mean free path within sample}} \text{ (optical thickness)} , \tag{2}$$

$$N_r = \frac{K_c E}{4\bar{\sigma} T_1^3} = \frac{\text{conductive heat flux}}{\text{radiative heat flux}} \text{ (radiation-conduction number)} , \tag{3}$$

and

$$\omega = \frac{\sigma}{E} = \frac{\text{scattering coefficient}}{\text{extinction coefficient}} \text{ (albedo)} , \tag{4}$$

where the parameters are defined in Table 1.

In the case of interest, the emissivities are equal to one and the extinction coefficient is equal to the absorption coefficient, that is, the pure absorption case for which the scattering coefficient and the albedo equal zero. Also, the thermal conductivity was assumed to be that of the continuous phase (i.e., air).

Table 1. Nomenclature

A, $A(E)$, $A(T_m)$, $A(\alpha)$, $A(\sigma)$	Constants in appropriate relationship
B, $B(E)$, $B(T_m)$, $B(\alpha)$, $B(\sigma)$	Constants in appropriate relationship
dL_i	Thickness of region i
E	Extinction coefficient, $E = \alpha + \sigma$
$E_n(\tau)$	nth-order integral exponential function of τ
F_s	Volume fraction of fibers in insulation
$G(\tau)$	Parameter defined by Eq. (8)
h	Heat transfer coefficient
$I(o)$	Intensity of light incident on a sample at $x = 0$
$I(x)$	Intensity of light emerging from a sample of thickness x
k_{air}	Thermal conductivity of air
k_{app}	Apparent thermal conductivity
k_c	Continuous-phase thermal conductivity
k_{eff}	Effective thermal conductivity, see Eq. (23)
k_r	Radiative conductivity, see Eq. (21)
k_{tot}	Total or enhanced thermal conductivity, see Eqs. (56) and (57)
L	Sample thickness
L_F	Full or actual-use thickness
L_R	Representative thickness for guarded hot-plate apparatus test specimens
M	Weighting factor in Eq. (62)
n	Refractive index τ
$n(\tau)$	Refractive index at
N	Number of increments within simulated sample
N_r	Radiation-conduction number defined by Eq. (3)
q_c	Conductive heat flux
q_r	Radiative heat flux
q_t	Total heat flux
$q_{t,i}$	Total heat flux through region i
Q	Parameter defined by Eq. (29), (30) or (31)
r	Correlation coefficient

Table 1. (Continued)

R	Thermal resistance
R_i	Thermal resistance of region i
R_L	Differential thermal resistivity
R_L^a	Apparent thermal resistivity, $1/k_{app}$
T	Absolute temperature
$T(\tau')$	Absolute temperature at τ'
$T_{Lin}(\tau)$	Absolute temperature for a linear temperature profile, $T_{Lin}(\tau) = T_2 + (\tau/\tau^\circ)(T_1 - T_2)$
T_m	Modified mean absolute temperature defined in Eq. (55)
T_1	Hot-plate absolute temperature
T_2	Cold-plate absolute temperature
T_1^*	Absolute temperature at interface between regions I and II
T_2^*	Absolute temperature at interface between regions II and III
x	Position
α	Absorption coefficient
β	Dimensionless slope at $\tau = 0$, see Eq. (12)
$\beta(\tau)$	$[\theta(\tau)]^4$
γ	Constant equal to 1.42089
δ	Convergence limit
ε	Emissivity
ε_1	Emissivity of hot plate
ε_2	Emissivity of cold plate
θ	Dimensionless or reduced temperature, T/T_1
$\theta(\tau)$	Dimensionless temperature at τ
$\theta^i(\tau)$	ith value of the dimensionless temperature at τ
θ_2	Dimensionless temperature at cold plate, T_2/T_1
σ	Scattering coefficient
$\bar{\sigma}$	Stefan-Boltzmann constant
τ	Dimensionless position, Ex
τ'	Variable of integration in Eqs. (7), (9), and (10)
τ°	Optical thickness, EL
τ_s	Parameter in Eq. (60), position at which $T = T_{Lin}$
ω	Albedo, Eq. (4)

The temperature profile for the pure absorption case with black boundaries was found by solution of the nonlinear integro-differential equation developed by Viskanta and Grosh,[10,11]

$$N_r \frac{d^2\theta(\tau)}{d\tau^2} = n^2(\tau)\theta^4(\tau) - 1/2\left[\beta(\tau)E_2(\tau) + \beta(\tau^\circ)E_2(\tau^\circ - \tau) + \int_0^{\tau^\circ} n^2(\tau')E_1(|\tau - \tau'|)\theta^4(\tau')\, d\tau'\right], \tag{5}$$

subject to boundary conditions

$$\theta(0) = \theta_2, \quad \theta(\tau^\circ) = 1.0 . \tag{6}$$

Viskanta and Grosh have shown that the dimensionless temperature $\theta(\tau)$ equals

$$\theta(\tau) = G(\tau) + \frac{1}{2N_r}\int_0^{\tau^\circ} n^2(\tau')\left\{-E_3(|\tau - \tau'|) + E_3(\tau') + \frac{\tau}{\tau^\circ}\left[E_3(\tau^\circ - \tau') - E_3(\tau')\right]\right\}\theta^4(\tau')\, d\tau' , \tag{7}$$

where

$$G(\tau) = \frac{1}{2N_r}\left(\beta(0)\left[-E_4(\tau) + \frac{\tau}{\tau^\circ}E_4(\tau^\circ) + \frac{1}{3}\left(1 - \frac{\tau}{\tau^\circ}\right)\right] + \beta(\tau^\circ)\left[\left(1 - \frac{\tau}{\tau^\circ}\right)E_4(\tau^\circ) - E_4(\tau^\circ - \tau) + \frac{1}{3}\frac{\tau}{\tau^\circ}\right] + 2N_r\left\{\theta(0) + \frac{\tau}{\tau^\circ}[\theta(\tau^\circ) - \theta(0)]\right\}\right). \tag{8}$$

Since a closed-form solution for Eq. (7) is not available, a numerical technique was used to obtain a solution for the temperature profile.[10,11]

Having determined the temperature profile, Viskanta and Grosh show that the total heat flux through the sample equals

$$q_t = \frac{k_c}{L}(T_1 - T_2) + 2\bar{\sigma}\Bigg(T_2^4\left[E_3(\tau^\circ) + \frac{1}{\tau^\circ}E_4(\tau^\circ) - \frac{1}{3\tau^\circ}\right] + T_1^4\left[-\frac{1}{\tau^\circ}E_4(\tau^\circ) - \frac{1}{2} + \frac{1}{3\tau^\circ}\right] + \int_0^{\tau^\circ} n^2(\tau')\Bigg\{E_2(\tau^\circ - \tau') + \frac{1}{\tau^\circ}\left[E_3(\tau^\circ - \tau') - E_3(\tau')\right]\Bigg\}T^4(\tau')\,d\tau'\Bigg) + \bar{\sigma}T_1^4 - 2\bar{\sigma}T_2^4E_3(\tau^\circ) - 2\bar{\sigma}\int_0^{\tau^\circ} n^2(\tau')E_2(\tau^\circ - \tau')T^4(\tau')\,d\tau' \,, \tag{9}$$

where the conductive heat flux is given by the first *two* terms in Eq. (9) and the heat flux due to radiation by the last three terms.[11] Combination of the integrals in Eq. (9) yields

$$q_t = \frac{k_c}{L}(T_1 - T_2) + 2\bar{\sigma}\Bigg\{T_2^4\left[\frac{1}{\tau^\circ}E_4(\tau^\circ) - \frac{1}{3\tau^\circ}\right] + T_1^4\left[-\frac{1}{\tau^\circ}E_4(\tau^\circ) + \frac{1}{3\tau^\circ}\right] + \int_0^{\tau^\circ} n^2(\tau')\frac{1}{\tau^\circ}\left[E_3(\tau^\circ - \tau') - E_3(\tau')\right]T^4(\tau')\,d\tau'\Bigg\} \,. \tag{10}$$

Equation (7) can be differentiated to show that

$$d\theta/d\tau = (1/2N_r)\Bigg(\beta(0)\left[E_3(\tau) + E_4(\tau^\circ)/\tau^\circ - 1/3\tau^\circ\right] + \beta(\tau^\circ)\left[-E_4(\tau^\circ)/\tau^\circ - E_3(\tau^\circ - \tau) + 1/3\tau^\circ\right] + (2N_r/\tau^\circ)\left[\theta(\tau^\circ) - \theta(0)\right] + \int_0^{\tau^\circ} n^2(\tau')\Bigg\{E_2(|\tau - \tau'|) + (1/\tau^\circ)\left[E_3(\tau^\circ - \tau') - E_3(\tau')\right]\Bigg\}\theta^4(\tau')\,d\tau'\Bigg) \tag{11}$$

By inspection of Eq. (11) one can show that the dimensionless slope β must satisfy the inequality

$$\beta = \left. \frac{d\left(\frac{\theta T_1 - T_2}{T_1 - T_2}\right)}{d\left(\frac{\tau}{\tau^\circ}\right)} \right|_{\tau = 0} \geq 1 \tag{12}$$

for a solution to be correct. An iterative technique different in detail but similar in principle to that used by Viskanta and Grosh[10,11] was developed in the current work for determination of the temperature profile and heat flux.

2.2 The Lii and Ozisik Analyses

An alternate solution technique was developed for the foregoing problem by Lii and Ozisik.[2] This solution is based on a normal mode expansion of the combined conduction and radiation heat transfer problem in an absorbing, emitting, and scattering medium. For further details of this analysis, the reader is referred to the original paper.[9]

2.3 Some Limiting Case Analysis (Thin, Thick, Remex)

Sparrow and Cess[12] show that for the optically thin limit, the mean free path of a photon, $1/E$, within an object is large compared to the thickness of the object, L. Thus

$$\tau^\circ = \frac{L}{1/E} = EL \ll 1 . \tag{13}$$

For this case, it was assumed that the radiant heat flux is not affected by the material and the conductive and radiative mechanisms do not interact.[12] The total heat flux through the object then equals

$$q_t = q_c + q_r , \tag{14}$$

where q_c is given by Fourier's law, which for a planar object of thickness L, constant properties, and unidirectional heat flow at steady state equals

$$q_c = k_c \frac{T_1 - T_2}{L} . \tag{15}$$

The radiant heat flux between two infinite parallel plates at T_1 and T_2 and with emissivities ε_1 and ε_2 equals

$$q_r = \frac{\bar{\sigma}\left(T_1^4 - T_2^4\right)}{\frac{1}{\varepsilon_1} + \frac{1}{\varepsilon_2} - 1} \tag{16}$$

Substitution of Eqs. (15) and (16) into Eq. (14) yields

$$q_t = k_c \frac{T_1 - T_2}{L} + \frac{\bar{\sigma}\left(T_1^4 - T_2^4\right)}{\frac{1}{\varepsilon_1} + \frac{1}{\varepsilon_2} - 1} . \tag{17}$$

For black plates $\varepsilon_1 = \varepsilon_2 = 1$, and Eq. (17) becomes

$$q_t = k_c \frac{T_1 - T_2}{L} + \bar{\sigma}(T_1^4 - T_2^4) . \tag{18}$$

When the limit of zero optical thickness is substituted into Eq. (12) and L'Hospital's rule is used to evaluate the indeterminant term that arises, Eq. (10) simplifies to Eq. (18).

Siegel and Howell[13] discuss the optically thick limiting case, where the dimensions of an object are large compared to the mean free path of a photon in the object,

$$\tau^\circ = \frac{L}{1/E} = EL \gg 1 , \tag{19}$$

and the photons that carry radiant energy within the object behave in a manner similar to photons in the conductive heat transfer process. The radiant heat flux is approximated by

$$q_r = -k_r \frac{dT}{dx} , \tag{20}$$

where for a gray medium the radiative conductivity k_r equals

$$k_r \simeq \frac{16}{3} \frac{n^2 \bar{\sigma} T^3}{\alpha} . \tag{21}$$

For combined conduction and radiation heat transfer,

$$q_t = -k_{\text{eff}} \frac{dT}{dx} , \tag{22}$$

where k_{eff}, the effective thermal conductivity, equals

$$k_{\text{eff}} = k_c + k_r . \tag{23}$$

Eliminating both k_{eff} between Eqs. (22) and (23) and k_r between the result and Eq. (21) and integrating the result yields the approximate total heat flux at steady state for one-directional heat flow in an optically thick slab,

$$q_t = k_c \frac{T_1 - T_2}{L} + \frac{4 n^2 \bar{\sigma} \left(T_1^4 - T_2^4 \right)}{3 \alpha L} . \tag{24}$$

Combining the total heat flux for the optically thin limiting case solution, Eq. (18), with the definition of the apparent thermal conductivity

$$k_{\text{app}} = q_t \, L / (T_1 - T_2) \tag{25}$$

yields a linear relationship between k_{app} and L for constant values of the plate temperatures:

$$k_{app} = k_c + \frac{\bar{\sigma}\left(T_1^4 - T_2^4\right)}{T_1 - T_2} L \ . \tag{26}$$

Substitution of the total heat flux for the optically thick limit, Eq. (24), into Eq. (25) shows that the asymptotic approach of the apparent thermal conductivity to an upper limit that is dependent on the absorption coefficient of the sample occurs at large sample thicknesses and high absorption coefficients. The asymptotic limit equals

$$k_{app} = k_c + \frac{4n^2 \bar{\sigma}\left(T_1^4 - T_2^4\right)}{3\alpha\left(T_1 - T_2\right)} \ . \tag{27}$$

A review of several methods for treating the effect of thickness on the apparent thermal properties of insulation was recently prepared by Rennex.[7] The models discussed by Rennex assume that interaction does not occur between conduction and radiation within the insulation and that the heat fluxes are additive.

Rennex discusses three solutions to the pure radiative heat transfer problem. At thermal or radiative equilibrium, the radiant heat flux between two infinite parallel plates at T_1 and T_2 separated by a gray medium equals

$$q_r = \frac{\bar{\sigma} Q \left(T_1^4 - T_2^4\right)}{1 + \left[(1/\varepsilon_1) + (1/\varepsilon_2) - 2\right] Q} \ . \tag{28}$$

An exact solution for Q developed by Heaslet and Warming[14] shows that for $\tau^\circ \gg 1$:

$$Q = \frac{4/3}{\tau^\circ + \gamma} \ , \tag{29}$$

where $\gamma = 1.42089$. The exponential-kernel approximation[12,15] to this problem yields

$$Q = \frac{4/3}{\tau^\circ + 4/3} , \tag{30}$$

while Rennex[7] proposes

$$Q = \frac{4/3}{\tau^\circ + 4/3\left[1 + 0.0657 \tanh (2\tau^\circ)\right]} \tag{31}$$

as a replacement for Eq. (29).

Assuming that the radiative and conductive heat fluxes do not interact and that the total flux equals the sum of the two independent fluxes, Rennex[7] developed the following equations for the effect of thickness on the apparent thermal conductivity by combining Eq. (29), (30), or (31) with Eq. (28) and Eqs. (28) and (15) with Eq. (14) to obtain q_t. This value of q_t was then inserted into Eq. (25) to yield

$$k_{app} = k_c + \frac{4\bar{\sigma}\bar{T}_m^3}{\frac{2}{\varepsilon} - 1 + \frac{3\tau^\circ}{4} + 0.0657} L , \tag{32}$$

$$k_{app} = k_c + \frac{4\bar{\sigma}\bar{T}_m^3}{\frac{2}{\varepsilon} - 1 + \frac{3\tau^\circ}{4}} L , \tag{33}$$

and

$$k_{app} = \frac{4\bar{\sigma}\bar{T}_m^3}{\frac{2}{\varepsilon} - 1 + \frac{3\tau^\circ}{4} + 0.0657 \tanh (2\tau^\circ)} L , \tag{34}$$

when it is assumed that $\varepsilon_1 = \varepsilon_2 = \varepsilon$ and $(T_1^4 - T_2^4)/(T_1 - T_2) \simeq 4T_m^3$.

For conduction and radiation with pure scattering ($\omega = 1$), interaction between the two modes of heat transfer does not occur,[1,2,12] and the conductive and radiative heat fluxes through the specimen are added to find

the total heat flux. For pure scattering, q_r is given by Eq. (28) and Q is given by Eq. (29) with τ° equal to σL.[12] It is therefore clear that Eq. (32), developed by Rennex,[7] is exact for combined conduction and radiation with pure scattering ($\omega = 1$).

For τ° greater than 2, $\tanh(2\tau^\circ)$ is equal to unity and thus Eqs. (32) and (34) are identical. As all cases of interest in this analysis have values of τ° greater than 2, only Eqs. (32) and (33) need to be discussed further. The only difference between Eqs. (32) and (33) is the constant in the denominator of Eqs. (29) and (30). The value 1.42089 was found for the exact solution,[14] while 1.3333 was found by the approximate technique.[12,15] As this is the only difference, only the exact solution which yields Eq. (32) will be used in subsequent analyses.

Since the thermal resistivity equals the inverse of the thermal conductivity, inverting Eq. (32) yields an expression for the apparent thermal resistivity. For the pure scattering case,

$$R_L^a = \frac{1}{k_{app}} = A(\sigma) + \frac{B(\sigma)}{\tau^\circ} , \tag{35}$$

where

$$A(\sigma) = \frac{1}{k_c \left\{ 1 + \frac{\frac{4}{3}(\frac{2}{\varepsilon} - 2) + \gamma}{\tau^\circ} \right\} + \frac{16\bar{\sigma}\bar{T}_m^3}{3\sigma}} \tag{36}$$

and

$$B(\sigma) = \frac{\frac{4}{3}(\frac{2}{\varepsilon} - 2) + \gamma}{k_c \left\{ 1 + \frac{\frac{4}{3}(\frac{2}{\varepsilon} - 2) + \gamma}{\tau^\circ} \right\} + \frac{16\bar{\sigma}\bar{T}_m^3}{3\sigma}} \tag{37}$$

2.4 Numerical Value of the Extinction Coefficient

In general, the extinction coefficient is a function of wavelength. To date, spectral or average extinction coefficients have not been measured for fibrous insulation for the wavelength range of interest, 3 to 20 μm. Pelanne[16] has, however, measured the percent transmittance of visible light, 0.4 to 0.7 μm, through fiberglass insulation, which can be converted to extinction coefficients using Beer's law:[13]

$$\frac{I(x)}{I(o)} = \exp(-Ex) \quad . \tag{38}$$

The results of these calculations, which represent an approximation to the values of interest, indicate that the extinction coefficient for fiberglass insulation lies in the range of 50 to 150 ft^{-1}. The optical thicknesses of the majority of insulation test specimens will, therefore, lie in the region where Eqs. (26) and (27) do not apply. Thus, we turn to the development of the relationship between the apparent thermal conductivity and sample thickness for intermediate optical thicknesses. For this purpose, the three-region approximation is a useful concept.

2.5 Development of a Three-Region Approximation

In principle, the effective thermal conductivity is an intensive property of a material. The radiation conduction approximation, defined by Eq. (20), however, is not a valid concept near the surfaces of an object. In this region, photons may pass through the object without interacting, a situation similar to the optically thin limit. It is, therefore, appropriate to approximate a planar insulation sample as an optically thin section of thickness dL_1 which is immediately adjacent to the hot surface in the test apparatus (region I), an optically thick central section (region II), and an optically thin section of thickness dL_2 which is immediately adjacent to the cold surface in the test apparatus (region III). The total heat fluxes through each region will then equal

$$q_{t,I} = k_c \frac{T_1 - T_1^*}{dL_1} + \bar{\sigma}\left(T_1^4 - T_1^{4*}\right) , \tag{39}$$

$$q_{t,II} = k_c \frac{T_1^* - T_2^*}{L_1 - dL - dL_2} + \frac{4\bar{\sigma}\left(T_1^{4*} - T_2^{4*}\right)}{3\alpha(L - dL_1 - dL_2)} , \tag{40}$$

and

$$q_{t,III} = k_c \frac{T_{2^*} - T_2}{dL_2} + \bar{\sigma}\left(T_{2^*}^4 - T_{2^*}^4\right) , \tag{41}$$

where T_1 and T_2 are the temperatures at the interfaces between regions I and II and II and III, respectively.

To simplify the analysis, it will be assumed that the thicknesses of regions I and III are equal. As some photons will be absorbed as soon as they enter the sample and others will travel well into the sample, an average thickness for regions I and III will be defined as the distance which will absorb one-half the incident radiant energy. According to Eq. (38), for the pure absorption case this thickness equals

$$dL_1 = dL_2 = -(\ln 0.5)/E = 0.69315/E . \tag{42}$$

Combining Eqs. (39) through (42) yields

$$T_1^* = T_1 - \left(T_1 - T_2\right)\frac{R_1}{R_1 + R_2 + R_3} , \tag{43}$$

$$T_2^* = T_2 + \left(T_1 - T_2\right)\frac{R_3}{R_1 + R_2 + R_3} , \tag{44}$$

and

$$q_t = \frac{T_1 - T_2}{R_1 + R_2 + R_3} , \tag{45}$$

where R_1, R_2, and R_3 are the thermal resistances of the regions. The values of these resistances are

$$R_1 = \frac{1}{(k_c\alpha/0.69315) + \bar{\sigma}\left(T_{1*}^2 + T_1^2\right)\left(T_{1*} + T_1\right)}, \tag{46}$$

$$R_2 = \frac{\tau^\circ - 2(0.69315)}{k_c\alpha + \frac{4}{3}\bar{\sigma}\left(T_{1*}^2 + T_{2*}^2\right)\left(T_{1*} + T_{2*}\right)}, \tag{47}$$

and

$$R_3 = \frac{1}{(k_c\alpha/0.69315) + \bar{\sigma}\left(T_{2*}^2 + T_2^2\right)\left(T_{2*} + T_2\right)}. \tag{48}$$

A relationship between the apparent thermal resistivity and specimen optical thickness was obtained by combining Eqs. (45) through (48) and the inverse of Eq. (25) for the pure absorption case. The resulting relationship is

$$R_L^a = \frac{1}{k_{app}} = A(\alpha) + \frac{B(\alpha)}{\tau^\circ} \tag{49}$$

where

$$A(\alpha) = \frac{1}{k_c + \left(4\bar{\sigma}/3\alpha\right)\left(T_{1*}^2 + T_{2*}^2\right)\left(T_{1*} + T_{2*}\right)}, \tag{50}$$

and

$$B(\alpha) = \frac{1}{(k_c/0.69315) + (\bar{\sigma}/\alpha)\left(T_{1*}^2 + T_1^2\right)\left(T_{1*} + T_1\right)} + \frac{1}{(k_c/0.69315) + (\bar{\sigma}/\alpha)\left(T_{2*}^2 + T_2^2\right)\left(T_{2*} + T_2\right)} - \frac{2(0.69315)/\alpha}{k_c + (4\bar{\sigma}/3\alpha)\left(T_{1*}^2 + T_{2*}^2\right)\left(T_{1*} + T_{2*}\right)}. \tag{51}$$

The foregoing analysis provides simplified equations, such as Eqs. (35) and (49), for interpretation of the dependence of the apparent thermal conductivity and resistivity of insulations upon measurement condition. These equations clearly show the dependency of the apparent thermal resistivity (or conductivity) on optical thickness and are finite for infinite τ°.

2.6 Effect of Temperature on Apparent Thermal Conductivity

The apparent thermal conductivity is dependent on temperature and strongly dependent on the term T_m^3 when the continuous-phase thermal conductivity, extinction coefficient, and plate emissitivity are approximately constant over the temperature range of interest and when the albedo equals one (pure scattering):

$$k_{app} = A(T_m) + B(T_m)T_m^3 . \tag{52}$$

The values of $A(T_m)$, $B(T_m)$, and T_m are established by the solution to the uncoupled heat transfer problem [Eq. (32)] with

$$A(T_m) = k_c , \tag{53}$$

$$B(T_m) = \frac{4\bar{\sigma}L}{(2/\varepsilon) - 1 + (3\tau^\circ/4) + 0.0657} , \tag{54}$$

and

$$T_m = \left[\frac{T_1^4 - T_2^4}{4(T_1 - T_2)}\right]^{1/3} = \left[\left(T_1^2 + T_2^2\right)\left(T_1 + T_2\right)/4\right]^{1/3} . \tag{55}$$

The dependence of the apparent thermal conductivity on temperature for the pure absorption case ($\omega = 0$), as given by the three-region approximation, appears to be more complicated than Eq. (52). As a first approximation, however, it can be assumed that k_{app} is linearly dependent on T_m^3 when the albedo equals zero.

2.7 Effect of Convection and Solid-Phase Conduction

Ideally we would like to include the effect of solid-phase conduction and convection in our solution efforts. At present, we can only estimate these effects. The contribution of solid-phase conduction to the apparent thermal conductivity of the insulation may be estimated by analyzing the insulation as an air-fiber composite. This composite will consist of a continuous phase with low thermal conductivity (i.e., air) and a randomly distributed phase with high condutivity (i.e., fibers). The thermal conductivity of the composite is given by the Maxwell-Eucken equation[17] and equals

$$k_{tot} = k_{air} \frac{1 + 2F_s}{1 - F_s} \quad . \tag{56}$$

Convection within the insulation will occur in parallel with conduction. Analysis of the parallel heat transfer problem yields an enhanced or total thermal conductivity,

$$k_{tot} = k_c\left(1 + \frac{hL}{k_c}\right) . \tag{57}$$

Rearrangement of Eq. (32) yields

$$k_{app} - k_c = \frac{4\bar{\sigma}T_m^3}{(2/\varepsilon) - 1 + (3/4)\tau^\circ + 0.0657} L . \tag{58}$$

Thus for the pure scattering case, the quantity $k_{app} - k_c$ will be unaffected by changing the value of the continuous-phase thermal conductivity [i.e., substituting k_{tot} from Eq. (56) or (57) for k_c]. If changing k_c does not affect $k_{app} - k_c$ (i.e., the apparent k_r), then for any total thermal conductivity,

$$k_{app}\Big|_{k_c=k_{tot}} = k_{app}\Big|_{k_c=0.18} + (k_{tot} - 0.18) \quad . \tag{59}$$

3. PROCEDURE

An iterative technique different in detail but similar in principle to that used by Viskanta and Grosh[10,11] was developed in the current work for determination of the temperature profile and heat flux. In this solution, the interval (0, L) was divided into N subintervals of equal length L/N and Eq. (7) was solved for the temperatures at the $N - 1$ interior points.

To begin a numerical calculation, values were selected for the absorption coefficient, thickness, refractive index, continuous-phase thermal conductivity, and hot- and cold-face absolute temperatures. The computer program is given in Appendix A2, and a flow chart of the program is shown in Fig. 1. The series approximation for the exponential integral functions[18] and the function $G(\tau)$ [Eq. (8)] were then evaluated, and an initial estimate for the dimensionless temperature profile was calculated from the equation

$$\frac{\theta(\tau) - \theta_2}{1 - \theta_2} = \frac{\left[(\beta - 1)(1 - \tau/\tau_s) + 1\right](\tau/\tau^\circ)}{1 + (\beta - 1)(1 - \tau/\tau_s)(\tau/\tau^\circ)} \quad . \tag{60}$$

Finally, the iterative solution was begun by calculating the $N - 1$ interior temperatures, $\theta^{i+1}(\tau)$, of Eq. (7) using the trapezoidal rule

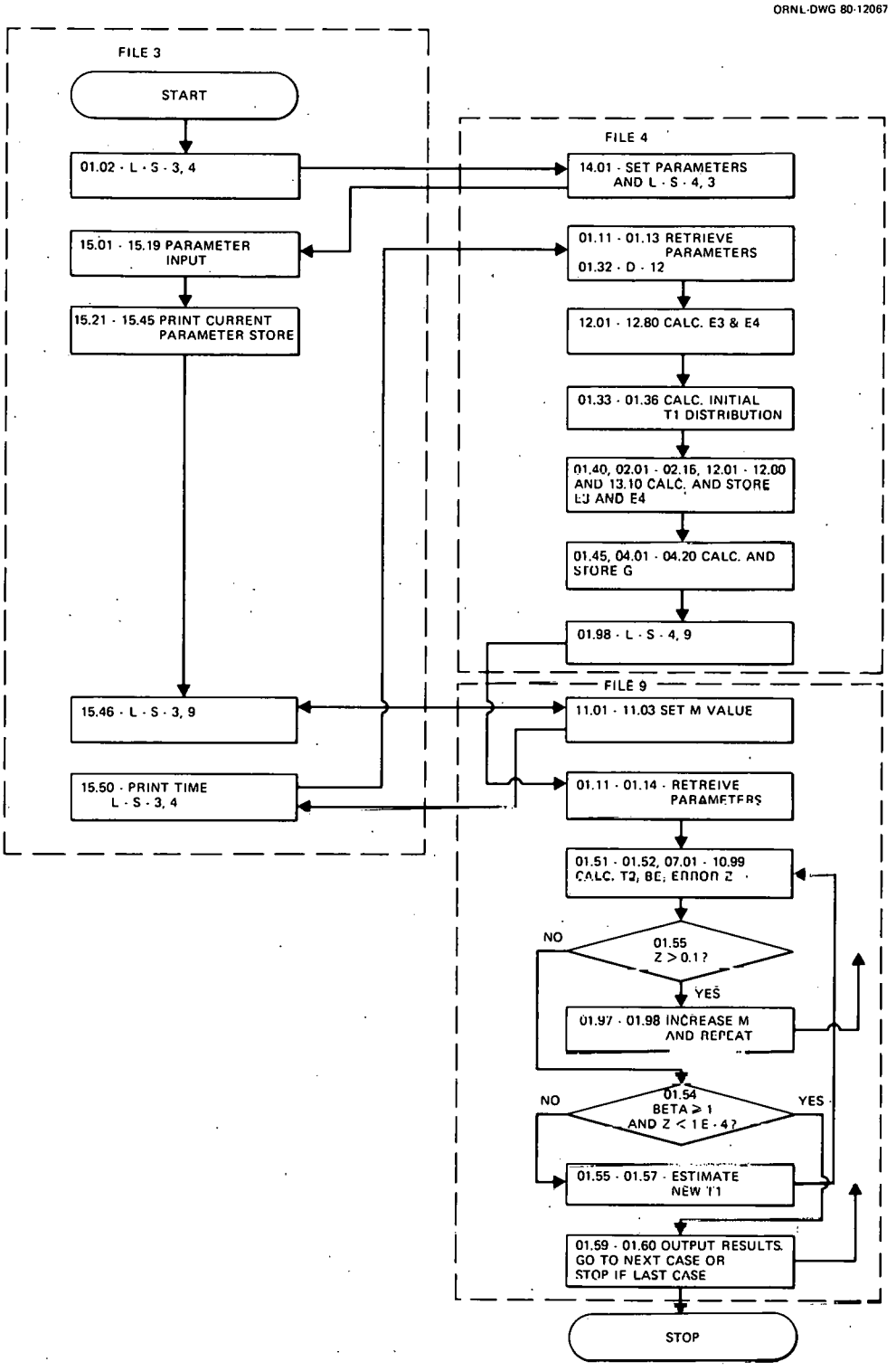

Fig. 1. Flow Chart for the Computer Program Used to Solve the Coupled Conductive-Radiative Heat Transfer Problem.

and the initial estimate for $\theta(\tau)$, $\theta^i(\tau)$, to evaluate terms on the right side of Eq. (7). A run was successfully terminated when Eq. (12) was satisfied and

$$\left| \frac{\theta^{i+1}(\tau) - \theta^{i}(\tau)}{\theta^{i}(\tau)} \right| \leq \delta \tag{61}$$

for all interior points. The convergence limit δ was usually set equal to 0.0001.

If either or both of the convergence criteria were not met, a weighted average of the current and previous values for $\theta(\tau)$ was used to produce a new estimate for the temperatures at the internal points. The new estimate equaled

$$\theta^{i+2}(\tau) = \frac{\theta^{i+1}(\tau) + M\theta^{i}(\tau)}{M + 1} , \tag{62}$$

where M was initially set equal to one. If, however, the calculated error became large, the computer set M equal to $2M + 1$ and Eq. (60) was used to restart the iterative procedure. The new estimates for $\theta(\tau)$ were used in Eq. (7), and the iterative process continued until both convergence criteria were met.

After successful convergence of the temperature profile was obtained, the trapezoidal rule was employed to calculate the total heat flux through the specimen and the apparent thermal conductivity using Eqs. (10) and (25).

4. RESULTS

Calculations were performed for guarded hot-plate conditions that would approximate building-insulation test conditions. In all cases, the refractive index of the sample was assumed to equal one. The effect of

the number of subintervals, convergence criterion (δ), absorption coefficient, thickness, continuous-phase thermal conductivity of the specimen, and hot- and cold-plate temperatures was investigated. Calculations for conditions identical to those studied by Viskanta[10,11] and Lii and Ozisik[2] were also run.

When the optical thickness τ° of the simulated sample was increased, the solution diverged in the initial calculations. At first the divergence problem was controllable for certain cases by increasing M (i.e., slowing the initial divergence of the solution). Increasing M, however, also slowed the convergence of the solution and led to long run times. In many cases, 100 iterations were made without convergence.

Extensive testing of the program indicated that if the number of subintervals was chosen such that

$$\frac{\tau^\circ}{N} = \frac{EL}{N} \leqslant 0.12 \ , \tag{63}$$

convergence of the program generally occurred with M equal to one. In the few cases where convergence did not occur, the origin of the problem was traced to a poor initial estimate for $\theta(\tau)$, which generally resulted from setting β in Eq. (60) too close to one. In these few cases, the program would have eventually converged. However, as each iteration takes approximatelly $11 \cdot (N/50)^2$ min on a PD/8e computer, these runs were stopped and restarted after increasing β.

The variation of the calculated total heat flux resulting from changing the size of convergence limit δ from 0.1 to 0.00001 was studied for a sample with an absorption coefficient of 100 ft^{-1}, a thickness of 0.25 ft, a continuous-phase thermal conductivity of 0.1800 Btu in./(h ft^2 °F), and hot- and cold-plate temperatures of 560 and 510°R, respectively. For δ equal to 0.001 and 0.00001, the calculated total heat fluxes were within 0.01% of the value obtained for δ equal to 0.0001, while for δ equal to 0.1 and 0.01, the calculated total heat fluxes were within 0.07% of the value for δ equal to 0.0001. While the run times for δ greater than 0.01 were substantially less than those for δ less than 0.001 (3.5 vs 10.5 h),

it was concluded that a small value for δ should be used to obtain the most accurate value for the total heat flux. Thus, in all ensuing runs, the convergence limit δ was set equal to 0.0001.

The relationships between the apparent thermal properties and sample thickness were investigated for hot- and cold-plate temperatures of 560 and 510°R, respectively. As the absorption coefficients for fibrous insulation are not known, calculations were performed for absorption coefficients between 0.001 and 1000 ft^{-1} at a thickness between 0.25 and 12 in. (0.0208 and 1 ft). The total heat fluxes, apparent thermal conductivities, and apparent thermal resistances for these calculations are given in Tables 2 through 4. The total heat fluxes through samples of thickness 0.042, 0.083, 0.292, and 1.0 ft are also plotted as functions of the absorption coefficient in Fig. 2. The apparent thermal conductivities are shown in Fig. 3. The apparent thermal resistances and resistivities for α = 50, 100, 150, and 200 ft^{-1} are shown in Figs. 4 and 5, respectively.

Examples of the nonlinearity of the temperature profiles obtained in the present solution technique are shown in Fig. 6. To highlight the nonlinearity of the profiles, the difference between the calculated temperature T and the temperature for a linear profile T_{Lin} are plotted versus the fraction of the optical thickness of the sample τ/τ°. In all cases, the temperature gradients at the hot and cold surfaces are steeper than those for uncoupled radiation and conduction. Substantial differences from the arithmetic-mean test temperature that would be expected at the midpoint of the specimen for uncoupled heat transfer $[(T_1 + T_2)/2]$ were also evident in all the cases studied.

The effect of varying the hot- and cold-plate temperatures on the apparent thermal conductivity was determined for sample thicknesses of 1 and 3 in. (0.0833 and 0.25 ft) with absorption coefficients of 50, 100, 150, and 200 ft^{-1}. A slight increase in the values of the apparent thermal conductivity was found when the test temperature difference, $T_1 - T_2$, was increased (see Table 5). Increasing the mean test temperature, with a constant 50°R temperature difference, however, resulted in a marked increase in the apparent thermal conductivity (see Table 6).

Table 2. Total Heat Flux Through a Sample with $n = 1$ and $k_c = 0.1800$ Btu in./(h ft^2 °F) Contained Between Black Plates at 560 and 510°R

α (ft^{-1})	Heat Flux, Btu/(h ft^2), for Various Sample Thicknesses, ft							
	0.0208	0.042	0.083	0.1667	0.292	0.5	0.75	1.0
0.001	88.6081	70.4637	61.6411	57.1019	55.1660	54.0902		53.3226
0.01	88.6010[a]	70.4502	61.6148	57.0494	55.0742	53.9329		53.0052
0.1	88.5355	70.3186	61.3561	56.5355	54.1733	52.3828		49.8406
1.0	87.9557	69.0594	58.9432	51.8902	46.4435	40.3550		31.1361
10.0	82.5162	59.3525	43.1394	29.1116	19.7842	12.9430	9.1395	7.0820
25.0	75.6693	49.2417	31.0268	17.9210	11.0037[b]	6.6915	4.5509	3.4480
50.0	67.7297	39.9042	22.6427	12.0500	7.0850	4.2055	2.8267	
75.0	62.3065	34.7119	18.8298	9.7325	5.6536[b]	3.3287		
100.0	58.3839	31.4447	16.6607	8.4994	4.9034			
125.0	55.4303	29.4128[c]	15.2161[d]	7.7335	4.4509[b]			
150.0	53.1351	27.6071	14.2557[d]	7.2157				
200.0	49.8217	25.6095[c]	13.0152[d]	6.5548				
500.0	42.3077	21.2300[c]	10.6591[d]					
1000.0	39.2559[e]	19.6532[e]						

[a] Thickness = 0.020833 ft.

[b] Thickness = 0.2917 ft.

[c] Thickness = 0.0417 ft.

[d] Thickness = 0.0833 ft.

[e] Thickness = 0.04167 ft.

Table 3. Apparent Thermal Conductivity of a Sample with $n = 1$ and $k_c = 0.1800$ Btu in./(h ft^2 °F) Contained Between Black Plates at 560 and 510°R

α (ft^{-1})	Thermal Conductivity, Btu in./h (ft^2 °F), for Various Sample Thicknesses, ft								
	0.0208	0.042	0.083	0.1667	0.292	0.5	0.75	1.0	∞ [a]
0.001	0.4430	0.7103	1.2279	2.2841	3.8660	6.4908		12.7974	
0.01	0.4430	0.7101	1.2274	2.2820	3.8596	6.4720		12.7213	
0.1	0.4427	0.7088	1.2222	2.2613	3.7965	6.2859		11.9617	
1.0	0.4391	0.6961	1.1742	2.0756	3.2548	4.8426		7.4727	17.0145
10.0	0.4119	0.5983	0.8593	1.1647	1.3064	1.5532	1.6451	1.6997	1.8634
25.0	0.3777	0.4964	0.6181	0.7170	0.7704[b]	0.8030	0.8192	0.8275	0.8534
50.0	0.3381	0.4022	0.4510	0.4821	0.4965	0.5047	0.5088		0.5167
75.0	0.3110	0.3499	0.3751	0.3894	0.3958[b]	0.3994		0.4045	
100.0	0.2915	0.3170	0.3319	0.3400	0.3436				0.3483
125.0	0.2767	0.2944[c]	0.3042[d]	0.3094	0.3116[b]				0.3147
150.0	0.2652	0.2783	0.2850[d]	0.2887					0.2922
200.0	0.2487	0.2563[c]	0.2602[d]	0.2622					0.2642
500.0	0.2112	0.2125[c]	0.2131						0.2137
1000.0	0.1962[e]	0.1967[f]							0.1968

[a] Calculated from Eq. (27).

[b] Thickness = 0.2917 ft.

[c] Thickness = 0.0417 ft.

[d] Thickness = 0.0833 ft.

[e] Thickness = 0.020833 ft.

[f] Thickness = 0.04167 ft.

Table 4. Apparent Thermal Resistance of a Sample with $n = 1$ and k_c = 0.1800 Btu in./(h ft^2) Contained Between Black Plates at 560 and 510°R

(ft^{-1})	Thermal Resistance, h ft^2 °F/Btu, for Various Sample Thicknesses, ft							
	0.0208	0.042	0.083	0.1667	0.292	0.5	0.75	1.0
0.001	0.564	0.710	0.811	0.876	0.906	0.924		0.938
0.01	0.564	0.710	0.811	0.876	0.908	0.927		0.943
0.1	0.565	0.711	0.815	0.884	0.923	0.955		1.003
1.0	0.568	0.724	0.848	0.963	1.077	1.239		1.606
10.0	0.606	0.842	1.159	1.718	2.527	3.863	5.471	7.060
25.0	0.661	1.015	1.612	2.790	4.544[a]	7.472	10.987	14.501
50.0	0.738	1.253	2.208	4.149	7.057	11.889	17.688	
75.0	0.802	1.440	2.655	5.137	8.844[a]	15.021		
100.0	0.856	1.590	3.001	5.883	10.197			
125.0	0.902	1.700[b]	3.286[c]	6.465	11.234[a]			
150.0	0.941	1.811	3.507[c]	6.929				
200.0	1.004	1.952[b]	3.842[c]	7.628				
500.0	1.182	2.355[b]	4.691[c]					
1000.0	1.274[d]	2.544[e]						

[a]Thickness = 0.2917 ft.

[b]Thickness = 0.0417 ft.

[c]Thickness = 0.0333 ft.

[d]Thickness = 0.020833 ft.

[e]Thickness = 0.04167 ft.

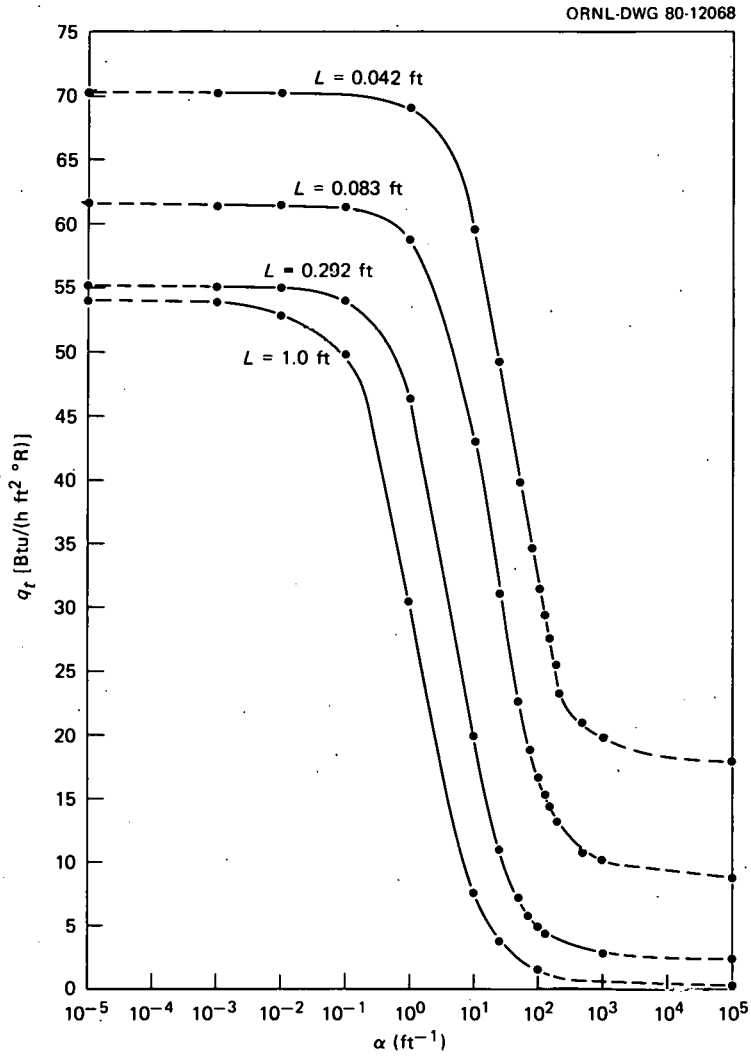

Fig. 2. Variation of Total Heat Flux with Absorption Coefficient, α (ft^{-1}), and Thickness for k_c = 0.1800 Btu in./(h ft^2 °F), T_1 = 560°R, and T_2 = 510°R.

Calculations were performed to determine how the apparent thermal conductivity of samples with an absorption coefficient of 75 ft^{-1} and sample thicknesses of 0.0883, 0.1667, and 0.2917 ft (1, 2, and 3.5 in.) changed as the thermal conductivity of the continuous phase was increased from 0.1800 to 0.1980 Btu in./(h ft^2 °F). As can be seen in Table 7, an increase in the continuous-phase thermal conductivity resulted in an increase of similar magnitude in the apparent thermal conductivity.

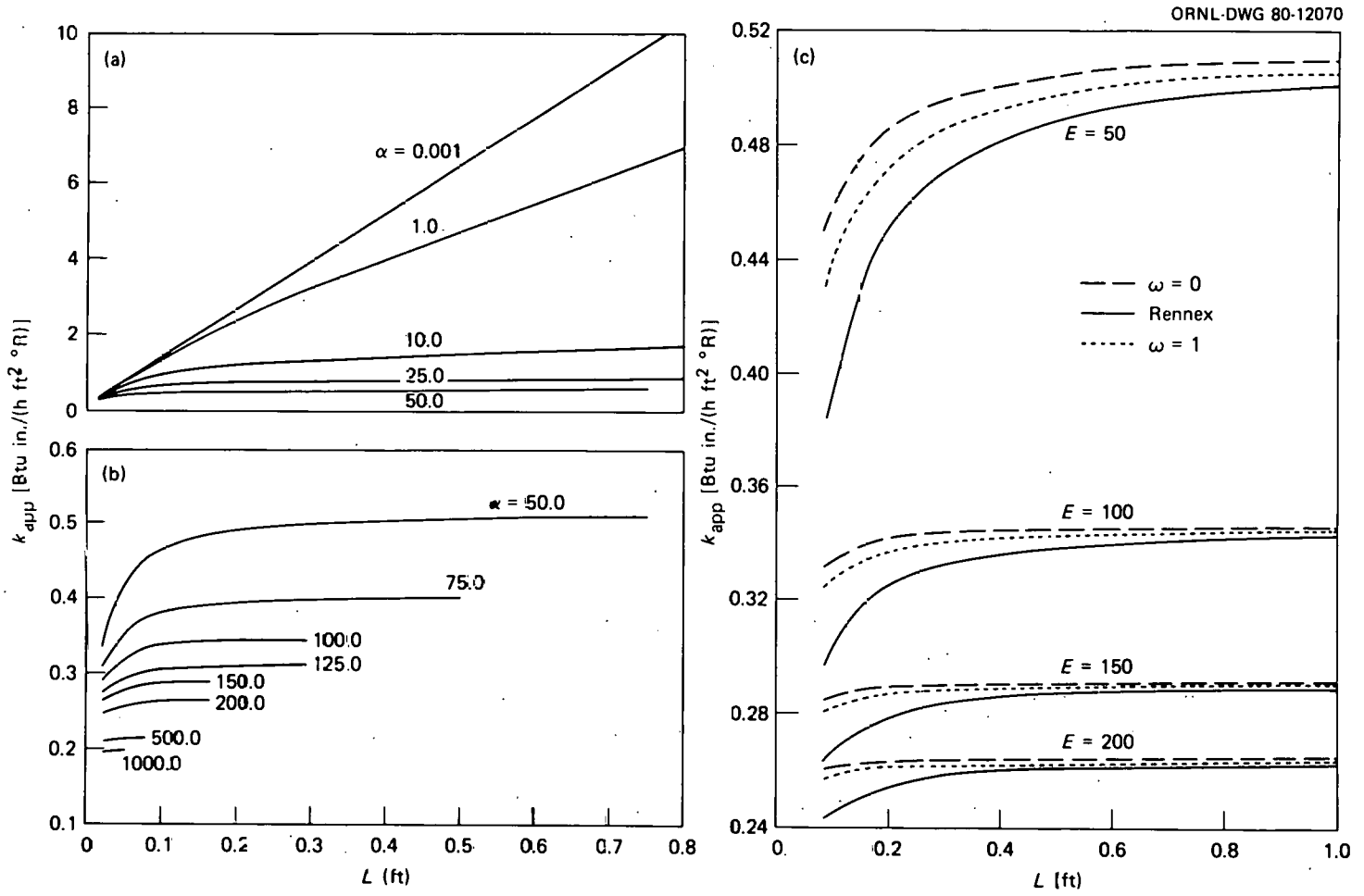

Fig. 3. Variation of Apparent Thermal Conductivity with Thickness and Absorption Coefficient, α (ft^{-1}), for k_c = 0.1800 Btu in./(h ft^2 °F), T_1 = 560°R, and T_2 = 510°R.

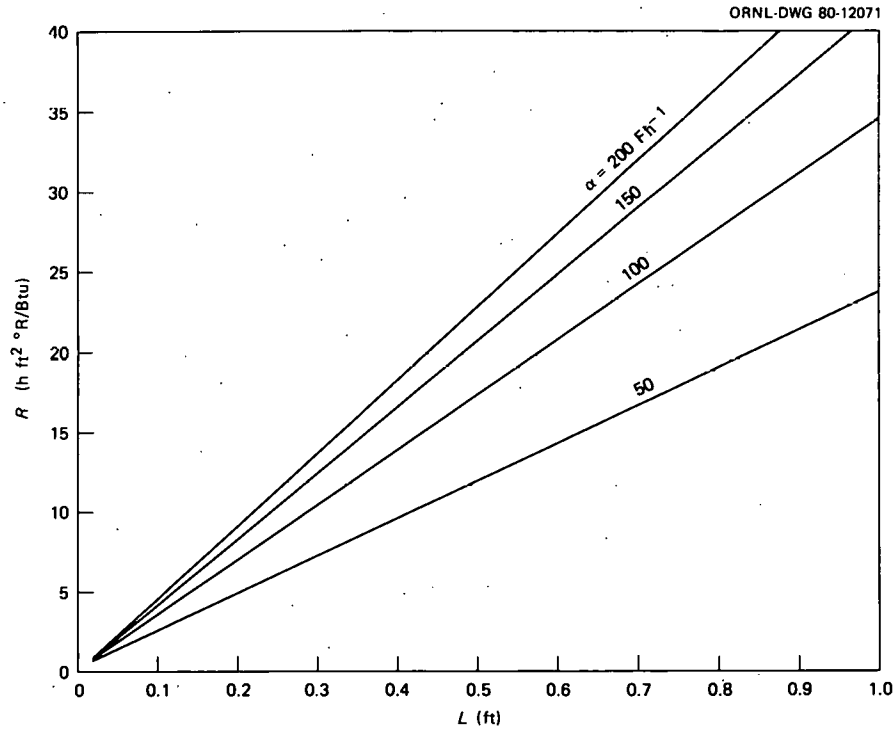

Fig. 4. Thermal Resistance vs Thickness for Absorption Coefficients of 50, 100, 150, and 200 ft^{-1}.

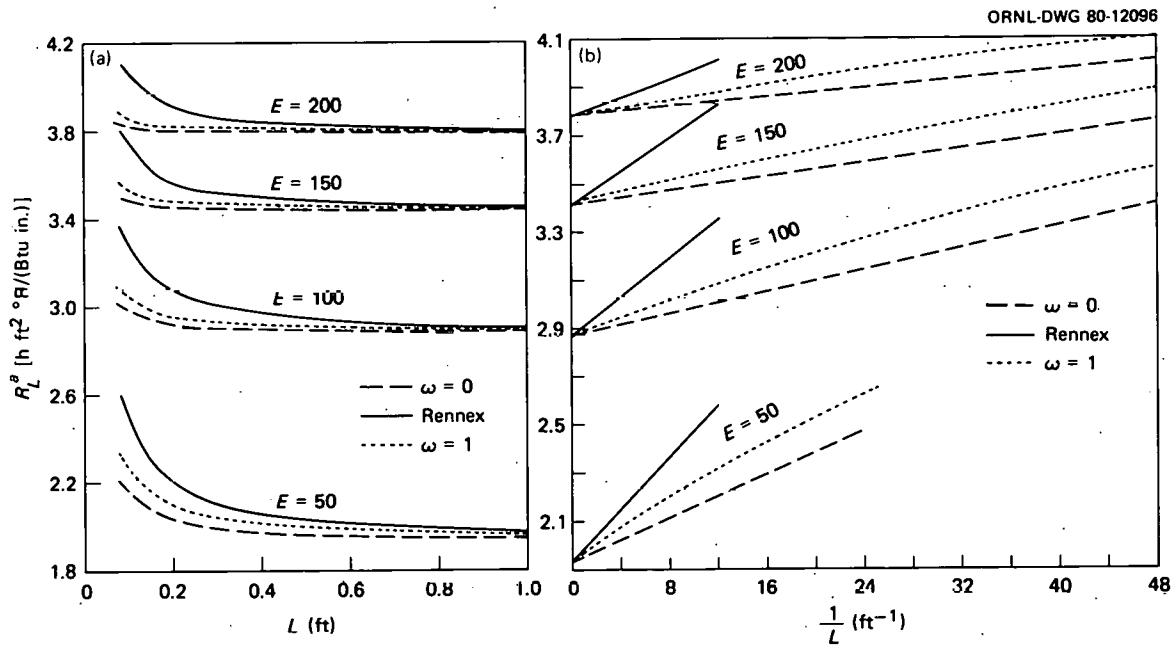

Fig. 5. Comparison of the Apparent Thermal Resistivity Obtained for the Pure Absorption Case ($\omega = 0$), the Pure Scattering Case ($\omega = 1$), and the Rennex (ref. 7) Extrapolation Equation for k_c = 0.1800 Btu in./(h ft^2 °F), T_1 = 560°R, T_2 = 510°R, and $\varepsilon = 1$.

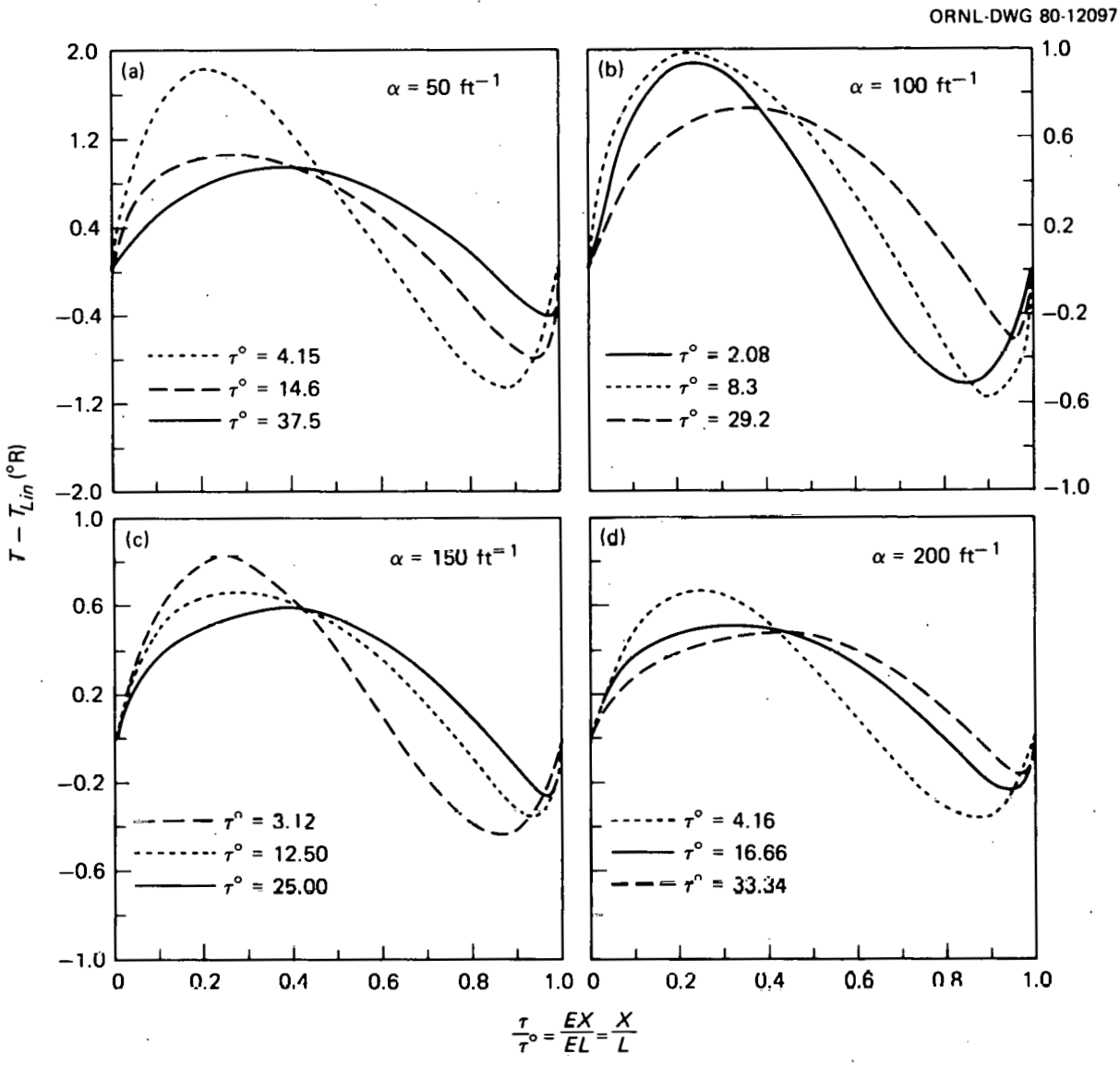

Fig. 6. Variation of the Calculated Temperature Profile from a Linear Profile for k_c = 0.1800 Btu in./(h ft^2 °F); T_1 = 560°R; T_2 = 510°R; and α = 50, 100, 150, and 200 ft^{-1} vs Dimensionless Position τ/τ°.

Table 5. Effect of Test Temperature Difference on the Apparent Thermal Conductivity[a]

T_1 (°R)	T_2 (°R)	T_m (°R)[b]	Thermal Conductivity, Btu in./(h ft^2 °F), at							
			α = 50 ft^{-1}		α = 100 ft^{-1}		α = 150 ft^{-1}		α = 200 ft^{-1}	
			L = 0.0833 ft	L = 0.25 ft	L = 0.0833 ft	L = 0.25 ft	L = 0.0833 ft	L = 0.25 ft	L = 0.0833 ft	L = 0.25 ft
550	520	535.14	0.4509	0.4927	0.3317	0.3426	0.2849	0.2897	0.2601	0.2627
560	510	535.39	0.4510	(0.4933)[c]	0.3319	0.3428	0.2850	0.2898	0.2602	0.2629
570	500	535.76	0.4519	0.4939	0.3323	0.3432	0.2853	0.2900	0.2604	0.2630
580	490	536.26	0.4521	0.4948	0.3327	0.3436	0.2856	0.2903	0.2606	0.2633
585	485	536.55	0.4532	(0.4953)[c]	0.3330	(0.3439)[c]	0.2858	0.2905	0.2608	0.2634
590	480	536.88	0.4537	0.4960	0.3333	0.3442	0.2860	0.2907	0.2609	0.2635
600	470	537.62	0.4549	0.4973	0.3339	0.3449	0.2864	0.2912	0.2612	0.2639

[a]Sample properties were n = 1, k_c = 0.1800 Btu in./(h ft^2 °F), and ϵ = 1.

[b]T_m defined by Eq. (55).

[c]Interpolated value.

Table 6. Effect of Mean Test Temperature on the Apparent Thermal Conductivity for a Test Temperature Difference of 50°F[a]

T_2/T_1	T_m (°R)	Thermal Conductivity, Btu in./(h ft^2 °F), at							
		α = 50 ft^{-1}		α = 100 ft^{-1}		α = 150 ft^{-1}		α = 200 ft^{-1}	
		L = 0.0833 ft	L = 0.25 ft	L = 0.0833 ft	L = 0.25 ft	L = 0.0833 ft	L = 0.25 ft	L = 0.0833 ft	L = 0.25 ft
435/485	460.5	0.3508	0.3576	0.2554	0.2621	0.2255	0.2234	0.2096	0.2112
475/525	500.4	0.3904	0.4252	0.2942	0.3030	0.2560	0.2598	0.2357	0.2378
505/555	530.4	0.4400	0.4819	0.3261	0.3367	0.2808	0.2854	0.2566	0.2592
510/560	535.4	0.4488	0.4919	0.3317	0.3426	0.2851	0.2898	0.2603	0.2629
515/565	540.4	0.4576	0.5020	0.3373	0.3486	0.2894	0.2943	0.2639	0.2666
545/595	570.4	0.5134	0.5661	0.3726	0.3860	0.3164	0.3222	0.2865	0.2897
585/635	610.3	0.5956	0.6607	0.4238	0.4406	0.3553	0.3626	0.3188	0.3227

[a]Sample properties were n = 1 and k_e = 0.03160 + 2.768 × 10$^{-4}T_m$ [Btu in./(h ft^2 °F)]. Also, ϵ = 1. Calculated using the three-region approximation.

Table 7. Effect of Continuous-Phase Thermal Conductivity[a] on the Apparent Thermal Conductivity for $\alpha = 75$ ft^{-1}

Length (ft)	Thermal Conductivity, Btu in./(h ft^2 °F)		
	k_c	k_{app}	$k_{app} - k_c$
0.0833	0.1800	0.3751	0.1951
	0.1809	0.3761	0.1952
	0.1858	0.3810	0.1952
	0.1980	0.3934	0.1954
0.1667	0.1800	0.3894	0.2094
	0.1809	0.3903	0.2094
	0.1858	0.3952	0.2094
	0.1980	0.4075	0.2095
0.2917	0.1800	0.3958	0.2158
	0.1809	0.3967	0.2158
	0.1858	0.4016	0.2158
	0.1980	0.4139	0.2159

[a]Test conditions were $n = 1$, $T_1 = 560$°R, $T_2 = 510$°R, and $\varepsilon = 1$.

Finally, several calculations were made to duplicate the results of Viskanta and Grosh[10,11] and Lii and Ozisik.[2] The conditions for these calculations assumed an arithmetic-mean test temperature of 535°R, $(T_1 + T_2)/2$, and a thermal conductivity of air equal to 0.1800 Btu in./(h ft^2 °F). The remainder of the conditions were then calculated from the values of the dimensionless parameters. The difference between the calculated total heat fluxes and the values given in the literature varied from less than 0.1% to slightly more than 4.5% (see Table 8).

Table 8. Results of Validation Calculations

α (ft^{-1})	L (ft)	q_{calc} [Btu/(h ft^2)]	q_{ref} [Btu/(h ft^2)]	Error (%)
		Optically Thin Limit[a]		
0.001	0.0208	88.6646	88.6654	0.001
	0.042	70.4637	70.4649	0.002
	0.083	61.6411	61.6439	0.005
	0.292	55.1660	55.1762	0.019
	0.5	54.0902	54.1077	0.032
	1.0	53.3226	53.3577	0.066
		Optically Thick Limit[a]		
25	1.0	3.4480	3.5557	3.03
50	0.75	2.8267	2.8705	1.53
75	0.5	3.3287	3.3705	1.24
125	0.2917	4.4509	4.4949	0.98
200	0.1667	6.5548	6.6030	0.74
500	0.0833	10.6591	10.6877	0.27
1000	0.0417	19.6532	19.6677	0.074
		Lii and Ozisik (ref. 2)		
280	0.00357	5,835.7[b]	5,833.7	0.034
56	0.0179	2,259.1[b]	2.262.4	−0.146
28	0.0357	1,821.3[b]	1,821.4	−0.0055
		Viskanta and Grosh (ref. 10)		
100	0.001	571,132[c]	571,100	0.006
10	0.01	78,842[c]	78,900	−0.086
1	0.1	29,600[c]	29,500	0.339
100	0.01	70,402[c]	71,400	−1.398
10	0.1	21,088[c]	21,900	−3.708
1	1.0	15,569[c]	16,300	−4.485
100	0.001	203,168[d]	203,800	−0.310
100	0.01	85.784[d]	89,900	−4.573
100	0.1	16,394[d]	16,300	0.577
		Viskanta (ref. 11)		
100	0.01	70,402[c]	70,377	0.050

[a]Conditions: T_1 = 560°R, T_2 = 510°R, and k_c = 0.015 Btu/(h ft °F).

[b]Conditions: T_1 = 1070°R, T_2 = 0°R, and k_c = 0.015 Btu/(h ft °F).

[c]Conditions: T_1 = 2000°R, T_2 = 1000°R, and k_c = 0.547 Btu/(h ft °F).

[d]Conditions: T_1 = 3000°R, T_2 = 1500°R, and k_c = 0.054 Btu/(h ft °F).

5. APPLICATIONS

The effects of thickness and other test conditions on the apparent thermal conductivity, resistivity, and resistance of insulation is widely recognized, although the magnitude of the effects is not well defined. To establish the magnitude of the effects, equations that relate the apparent thermal properties of insulation to the test conditions were developed in an earlier section. To bracket the magnitude of the effects for tests performed on building insulations, the results for the numerical solution and the three-region approximation to the coupled heat transfer problem are compared with the limiting solutions for which no interaction is assumed between conduction and radiation. The accuracy of the numerical solution of the coupled heat transfer problem which is used to model the measurement of the apparent thermal conductivity in a guarded hot plate must, however, be discussed first.

5.1 Analysis of Errors

To assess the accuracy of the numerical solution used in this work, the solution results should be compared to the results of an analytical solution to the same problem. An analytical solution to the problem of interest is, however, not available. Thus, the results of the numerical solution can only be compared with the limiting solutions for the optically thin and thick cases; the results reported by Viskanta and Grosh,[1,10,11] which were obtained using a similar numerical technique; and the results of the Lii and Ozisik[2] method.

When the total heat fluxes calculated using the numerical solution technique for $\tau^\circ < 10^{-3}$ are compared with the values calculated from Eq. (18), the agreement between the results obtained from the numerical solution and those calculated using Eq. (18) is better than 0.07% in all cases, as shown in the first six rows of Table 8.

While the optically thick limit is generally considered to be applicable for optical thicknesses greater than 10, rows 7 through 13 of Table 8 indicate that the total heat flux obtained from the present

iterative solution does not approach the limiting value until τ° is greater than 40. At this point, however, the agreement is better than 0.3%. It must be remembered that Eqs. (23) and (24) are approximations and that exact agreement betweeen the present iterative solution and the approximate solution will only occur at infinite optical thicknesses. The fact that the iterative and approximate solutions approach the same value at τ° values as low as 40 is further evidence that the present iterative solution technique yields correct results.

An alternate solution technique based on a normal-mode expansion of the combined conductive and radiative heat transfer problem in an absorbing, emitting, and scattering medium has been developed by Lii and Ozisik[2] (see Sect. 2.2). The total heat flux through an infinite slab was calculated for several cases, including that of black plates ($\varepsilon = 1$) and no scattering ($\omega = 0$), for an optical thickness of one. Results from Lii and Ozisik and from the present work are shown in Table 8 (rows 14 through 17). As can be seen from the table, the agreement is better than 0.04% for two cases and 0.15% for the third case.

A final check on the accuracy of the present iterative solution involved repeating some of the cases reported by Viskanta and Grosh.[10] All the Viskanta and Grosh cases were not repeated, as disagreements of more than 4.5% occurred for some of the first cases treated (see Table 8). Thus, a careful check of all the data reported by Viskanta and Grosh[1,10,11,19] was undertaken in an attempt to explain these discrepancies before redoing additional cases.

When the first three Viskanta and Grosh publications[10,11,19] were compared, it was found that the total heat fluxes for similar cases in all three agreed. However, it was also seen that the conductive and radiative heat fluxes did not agree in many cases. Furthermore, in the cases for which the largest disagreements occurred between Viskanta and Grosh's results and the current work, the largest disagreements also occurred for the conduction and radiation heat fluxes in Viskanta and Grosh's own publications.

It appears that Viskanta and Grosh's problem arises from the procedure used to calculate the conduction heat flux. Their original work[11] clearly stated that the conductive heat flux equals the first *two* terms

of Eq. (9). However, in their first paper, it appears that only the first term was used. This error was probably carried over into their second paper,[19] which was prepared concurrently with their first paper.

A further comparison of the first three works[10,11,19] with a later paper[1] shows that the error may have been corrected. This comparison showed disagreement of the total heat fluxes for identical cases in Viskanta and Grosh's own papers but excellent agreement of the last paper's results with the present work (see the last row of Table 8). Further comparisons with Viskanta and Grosh's work were not attempted, as it was not possible to state with complete certainty which of their results were correct.

Based on the excellent agreement between the total heat fluxes obtained from the present iterative solution and the values calculated for the optically thin and thick limits ($\tau^\circ \ll 1$ and $\tau^\circ > 40$) and the agreement with the results reported by Lii and Ozisik[2] and Viskanta,[1] it was concluded that an error of less than 0.1% should be expected between the present results and the value of the total heat flux.

5.2 Thickness Effect

The effect of sample thickness on the apparent thermal conductivity is shown in Fig. 3. The linear behavior for small sample thicknesses and low absorption coefficients is easily explained by the optically thin limiting case of Eq. (26). As the optical thickness increases, the apparent thermal conductivity asymptotically approaches a limiting value, Eq. (27). The intermediate regime will be discussed in terms of the apparent thermal resistivity, as the three-region approximation shows a linear dependence of R_L^a on $1/\tau^\circ$.

Equations (43) through (48) are easily solved using an iterative technique as indicated in Appendices A3 and A4. The iteration quickly converges when T_1^* and T_2^* are set equal to T_1 and T_2, respectively, in Eqs. (46), (47), and (48). The values of R_1, R_2, and R_3 are then used to find T_1^* [Eq. (43)] and T_2^* [Eq. (44)]. The process is repeated until the values of T_1^* and T_2^* used in Eqs. (46), (47), and (48) approximate those

obtained from Eqs. (43) and (44). [A convergence limit similar to Eq. (61) may be employed to establish a criterion for successful convergence.] The total heat flux through the sample is then calculated using Eq. (45), and the apparent thermal resistivity or conductivity is calculated.

As it is not possible to have a negative thermal resistance, it is clear from Eq. (47) that the minimum optical thickness of the sample must be 1.3863. However, as region II is assumed to be optically thick, it is likely that this three-region approximation will only be valid for optical thicknesses considerably greater than 1.3863. Table 9 shows the values of the apparent thermal conductivities calculated using the three-region approximation and the percent difference between these values and the apparent thermal conductivities calculated for corresponding conditions using Eqs. (10) and (25). As can be seen in this table, the largest error is less than 2%. For a greater than or equal to 50 ft^{-1} and τ° greater than 4, the largest error is only —0.55%. The three-region approximation is an excellent one for the analysis of the coupled conduction and radiation heat transfer problems of interest.

The apparent thermal resistivities obtained from the numerical iterative solution are plotted versus the reciprocal of the sample thickness in Fig. 5. As can be seen from this figure and the results of the least squares analyses given in Table 10, R_L^a varies linearly with $1/\tau^\circ$ as suggested by Eq. (49) for $\tau^\circ > 2$.

The data used in the analyses in this and following sections were obtained from the numerical solution for optical thicknesses less than 40 and from the three-region approximation for τ° greater than 40. The numerical solution of Eqs. (7) and (10) was limited to optical thicknesses less than 40 because of computer limitations.

A comparison of Eq. (50) with the definition of the effective thermal conductivity suggests that

$$A(\alpha) \simeq \frac{1}{k_{eff}} . \tag{64}$$

Table 9. Apparent Thermal Conductivities[a] Predicted by the Three-Region Approximation for a Sample with n = 1 and k_c = 0.1800 Btu in./(h ft^2 °F) Contained Between Black Plates at 560 and 510°R

α (ft^{-1})	Thermal Conductivity, Btu in./(h ft^2 °F), for Various Sample Thicknesses, ft							
	0.0208	0.042	0.083	0.1667	0.292	0.5	0.75	1.0
25			0.6064 (−1.89)	0.7096 (−1.03)	0.7649 (−0.72)	0.7994 (−0.44)	0.8166 (−0.31)	0.8255 (−0.24)
50		0.3973 (−1.22)	0.4485 (−0.55)	0.4804 (−0.46)	0.4953 (−0.28)	0.5040 (−0.13)	0.5082 (−0.13)	0.5103
100	0.2900 (−0.51)	0.3168 (−0.059)	0.3316 (−0.077)	0.3398 (−0.067)	0.3434 (−0.059)	0.3455	0.3464	0.3469
150	0.2656 (+0.12)	0.2784 (+0.037)	0.2851[b] (+0.028)	0.2866 (−0.025)	0.2902[c]	0.2910	0.2914	0.2916
200	0.2492 (+0.19)	0.2565[d] (+0.65)	0.2603[b] (+0.023)	0.2622 (0.00)	0.2630[c]	0.2635	0.2637	0.2638
500	0.2114 (+0.075)	0.2125[d] (+0.019)	0.2131[b] (−0.010)	0.2134	0.2135[c]	0.2136	0.2136	0.2136
1000	0.1963[e] (+0.013)	0.1966[f] (+0.003)	0.1967[b]	0.1968	0.1968[c]	0.1968	0.1968	0.1968

[a]Values in parentheses are percent difference of two solutions.

[b]Thickness = 0.0833 ft.

[c]Thickness = 0.2917 ft.

[d]Thickness = 0.0417 ft.

[e]Thickness = 0.02083 ft.

[f]Thickness = 0.04167 ft.

Table 10. Least Squares Analysis Results

E (ft^{-1})	$1/k_{eff}$ [h ft^2 °F/(Btu in.)][a]	$A(E)$	$B(E)$	r
	$\omega = 0, \varepsilon = 1, \tau^\circ > 2$			
10	0.5366	0.5344	0.5463	0.99995
25	1.1718	1.1713	0.9274	0.99999
50	1.9354	1.9350	1.1589	0.99996
75	2.4724	2.4717	1.2147	0.99997
100	2.8707	2.8715	1.1691	0.99993
125	3.1779	3.1781	1.1348	0.99999
150	3.4220	3.4216	1.0863	0.99999
200	3.7854	3.7848	0.9797	0.99998
500	4.6801	4.6798	0.5679	0.99977
1000	5.0804	5.0803	0.3165	0.99992
	$\omega = 1, \varepsilon = 1, \tau^\circ > 2, L > 0.0833$ ft			
10	0.5366	0.5403	0.6481	0.99996
25	0.1718	1.1840	1.1346	0.99946
50	1.9354	1.9424	1.5856	0.99962
75	2.4724	2.4769	1.7554	0.99972
100	2.8707	2.8737	1.7982	0.99979
125	3.1779	3.1800	1.7809	0.99983
150	3.4220	3.4235	1.7349	0.99987
200	3.7854	3.7863	1.6118	0.99990
500	4.6801	4.6802	1.0162	1.0
1000	5.0804	5.0804	0.6071	1.0

[a]Calculated from Eq. (27).

The comparison of the regression analysis intercepts $A(\alpha)$ and the inverse of k_{eff} calculated from Eq. (23) shows that the intercept of Eq. (49) equals the inverse of the effective thermal conductivity (see Table 10). A comparison of Eq. (49) for the coupled conduction and radiation heat transfer case ($\omega = 0$) and Eq. (35) for the uncoupled conduction and radiation case ($\omega = 1$) is shown in Fig. 5 for black plates ($\varepsilon = 1$) and extinction coefficients of 50, 100, 150, and 200 ft^{-1}. This figure clearly shows that a linear relationship exists between the apparent thermal resistivity and $1/\tau^\circ$ for both the coupled and the uncoupled cases. Furthermore, Fig. 5 shows that the intercepts for both cases equal the inverse of the effective thermal conductivity and that the only difference

between the linear relationships predicted by the two cases results from different values of the slopes. A comparison of the values of the slopes, $B(\alpha)$ and $B(\sigma)$, is shown in Fig. 7 and Table 10. The pure absorption case ($\omega = 0$) has the smaller slope.

Finally, Rennex[7] correctly concludes that the apparent thermal resistance has a linear dependence on sample thickness as the sample thickness approaches infinity. As the apparent thermal resistivity equals the apparent thermal resistance divided by thickness, extension of Rennex's analysis also shows that R_L^a is inversely dependent on τ°,

$$R_L^a = \frac{R}{L} = \frac{1}{k_{app}} = A + \frac{B}{L} , \tag{65}$$

$$A = \frac{1}{k_c\left(1 + \frac{k_s}{k_c}\right)} , \tag{66}$$

and

$$B = \frac{(2/\varepsilon - 1 + 0.0657)/4\bar{\sigma}T_m^3}{k_c/k_s + 1} , \tag{67}$$

where

$$k_s = \frac{16\bar{\sigma}T_m^3}{3\sigma} . \tag{68}$$

The slope obtained from Rennex's equation is incorrect for sample thicknesses of less than 1 ft. As can be seen in Fig. 5, Rennex's equation yields the correct intercept for infinite thickness, $1/L = 0$, but has a slope that is much greater than the correct slope for the pure scattering case ($\omega = 1$). This difference resulted because Rennex developed the relationship assuming infinite thickness, which is inappropriate for the building-insulation case. This has subsequently been changed to yield a value for B [Eq. (67)] that agrees with B [Eq. (37)].[20]

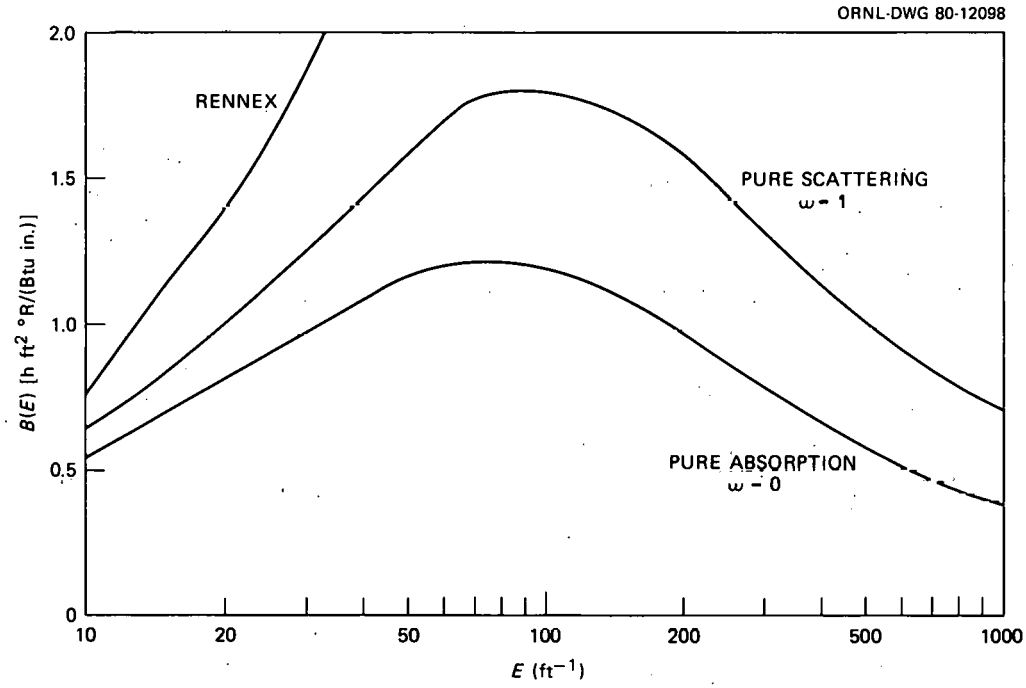

Fig. 7. Comparison of the Slopes for Extinction Coefficients Between 10 and 1000 ft^{-1} in the Relationship Between the Apparent Thermal Resistivity and $1/\tau^{\circ}$ for the Pure Absorption Case ($\omega = 0$), the Pure Scattering Case ($\omega = 1$), and the Rennex (ref. 7) Relationship.

5.3 Temperature Effect

The plate temperatures in a guarded hot-plate apparatus establish the test temperature difference ($\bar{T}_1 - T_2$) and the modified-mean absolute test temperature (T_m). The effect of these parameters on the measured results was examined in the theory section.

To test the validity of the assumptions made in the theory section, calculations were performed at several mean test temperatures for 1- and 3-in.-thick (0.0833- and 0.25-ft) samples with absorption coefficients of 50, 100, 150, and 200 ft^{-1} (see Table 6). The resulting apparent thermal conductivities were then fitted by the method of least squares to a linear relationship similar to Eq. (52) for each value of α and L. The correlation coefficient was determined. Even though continuous-phase thermal conductivity used in the calculations were allowed to vary with T_m, linear relationships similar to Eq. (52), but having different intercepts and slopes, fit each set of data with a correlation coefficient of 0.998 or better.

Calculations were also performed to establish the effect of the test temperature difference on k_{app} (see Table 5). Prior to these calculations, it was believed that the mean test temperature could be approximated as

$$T_m \simeq \frac{T_1 + T_2}{2} \quad . \tag{69}$$

However, least squares analyses of these results showed that the slight but significant variation of k_{app} shown in Table 5 resulted from $T_1 - T_2$ changing T_m, Eq. (55), even though the approximate value of T_m, Eq. (69), was constant. Thus, the test temperature difference does not have a direct effect on the measured value of k_{app}, but rather an indirect effect that results from the dependence of T_m on T_1 and T_2 as shown in Eq. (55).

5.4 Emissivity Effect

The emissivities of the plates in a guarded hot-plate apparatus affect the measured value of the apparent thermal conductivity. The plate emissivity effect is examined in this section.

The plate emissivities were easily incorporated into the analysis of the uncoupled conduction and radiation heat transfer problem ($\omega = 1$). The results of this analysis [Eq. (32)] clearly show the relationship between the apparent thermal conductivity and the emissivity of the plates.

The iterative solution and the three-region approximation assumed that the bounding surfaces were black ($\varepsilon = 1$). Viskanta[1] has, however, reported a set of results that shows the effect of emissivity on the total heat flux for coupled conduction and radiation. These values may be inserted into Eq. (25) to show the effect of the emissivity on the apparent thermal conductivity of a sample with an optical thickness of one. As can be seen in Table 11, decreasing the plate emissivity decreases the calculated apparent thermal conductivity. Furthermore, the decrease is larger for the pure scattering case than for the pure absorption case or, conversely, the increase in the apparent thermal resistivity is more for the pure scattering case than for the pure absorption case for

Table 11. Effect of Albedo and Emissivity on the Apparent Thermal Conductivity for $N_{\mathcal{P}} = 1.0$, $\tau^\circ = 1.0$, and $\Theta_2 = 0.5$

ε	Apparent Thermal Conductivity,[a] Btu in./(h ft^2 °F)		
	$\omega = 0$[b]	$\omega = 0.5$	$\omega = 1.0$[c]
1.0	0.2316	0.2295	0.2273
0.75	0.2215	0.2185	0.2143
0.5	0.2127	0.2085	0.2025
0.25	0.2055	0.1990	0.1914
0.1	0.1994	0.1937	0.1847

[a]Calculated from dimensionless heat fluxes given by Viskanta (ref. 1) assuming $T_1 = 713.33$ °R and $k_c = 0.1800$ Btu in./(h ft^2 °F).

[b]Pure absorption.

[c]Pure scattering.

identical test conditions. As the intercepts in the relationships between R_L^a and $1/\tau^\circ$ equal the inverse of k_{eff} and this value is independent of ε, the larger increase in R_L^a for the pure scattering case must correspond to a larger increase in the slope, $B(\sigma)$.

5.5 Conduction in the Solid Phase and Convection Effect

In an attempt to include solid-phase conduction and convection in the present analysis, the continuous-phase thermal conductivity can be enhanced as shown in the theory section to include contributions due to these other mechanisms. The enhanced value for the thermal conductivity is then used in the calculations, in place of the value for air, to determine what effect these mechanisms have on the apparent thermal conductivity.

For insulations with densities between 0.37 and 1.56 lb/ft^3, Eq. (56) yields total thermal conductivities that are 0.5 to 3.2% larger than the value for air. Values for k_{tot} equal to 1.005, 1.032, and 1.1 k_{air} (the case for $hL/k_c = 0.1$) were used in place of k_{air} for several calculations

(see Table 7). As can be seen from the last column in the table, changing k_c does not affect $k_{app} - k_c$ (i.e., k_r). Thus, the assumption of Eq. (58) is applicable. These calculations show that k_r does change with thickness.

5.6 Albedo Effect

Prior sections have examined the effect of thickness, temperature, emissivity, and continuous-phase thermal conductivity on the apparent thermal conductivity or resistivity. These analyses were based on the solutions for the pure absorption case ($\omega = 0$) and the pure scattering case ($\omega = 1$). However, both absorption and scattering occur in insulation, and the actual case of importance has an albedo somewhere between zero and one.

Viskanta[1] has developed a solution for coupled conduction and radiation in an absorbing and scattering medium. Combination of Viskanta's results and Eq. (25) permits the dependence of the apparent thermal conductivity on the albedo to be demonstrated for τ^* and $N_r = 1.0$, $\theta_2 = 0.5$, and various values of the plate emissivity. As shown in Table 11, the apparent thermal conductivity for an intermediate value of the albedo ($\omega = 0.5$) consistently falls between the values for the albedo equal to 0 and 1.0. Since this trend occurs for any combination of thickness, temperature, emissivity, and continuous-phase thermal conductivity which yields the specified values of the dimensionless parameters, the effects of thickness, temperature, emissivity, and continuous-phase thermal conductivity (resistivity) which were developed in the previous sections for $\omega = 0$ and 1.0 bracket the effect of these variables on the apparent thermal conductivity for an albedo between 0 and 1.0.

5.7 Full-Thickness Calculations

Definitions of the thermal properties and a method for establishing the minimum or representative thickness for which these properties can be defined for low-density materials are set forth by the ASTM[3] in C177-76. (A portion of this specification is reprinted in Appendix A1.) The ASTM method for establishing the representative thickness and R-values are used

by the FTC.[5] These specifications are discussed in this section. It is also shown how the equations that represent the effect of thickness on the apparent thermal resistivity for the pure scattering calculation [Eq. (35)] and for the pure absorption calculation [Eq. (49)] may be used to establish the value of the representative thickness and the full-thickness resistance of building insulation.

The ASTM C177-76 specification requires that the thermal resistance be a linear function of the sample thickness and that the function have a value of zero at zero thickness. Further, the specification recognizes that a minimum sample thickness may exist above which the definitions apply and a procedure for estimating this thickness is set forth (see Sect. XI.4.6 in Appendix A1).

For a material whose thermal properties are a function of thickness, the ASTM specification appears to define two thermal resistivities — an average or mean thermal resistivity and an instantaneous or differential thermal resistivity. The mean thermal resistivity is defined as the slope of the resistance versus thickness curve, which is assumed to go through zero at zero thickness; that is,

$$R_L^a = \frac{R(L) - R(0)}{L - 0} = \frac{R(L)}{L} . \tag{70}$$

The differential thermal resistivity is the incremental change in the resistance for an incremental increase in thickness,

$$R_L = \frac{R(L_2) - R(L_1)}{L_2 - L_1} = \frac{\Delta R}{\Delta L} . \tag{71}$$

In the limit of L_2 approaching L_1, the differential thermal resistivity equals the derivative of the resistance function:

$$\lim_{L_2 \to L_1} R_L = \frac{dR}{dL} . \tag{72}$$

Then, according to C177-76, the representative thickness is the minimum sample thickness for which the differential thermal resistivity is within 2% of the mean thermal resistivity of the largest sample that is to be characterized or that can be measured in the test apparatus.

The FTC final rule[5] requires that all measurements for the resistance of building insulation be made at a specimen thickness greater than that for which the apparent thermal resistivity of the material does not change by more than 2% with thickness increases to full thickness. The FTC final rule does not specify whether the mean or the differential thermal resistivity must be used to establish the representative thickness L_R. While it is believed that the intent of the FTC rule was to require that the mean value be used, it will be shown that using the differential thermal resistivity leads to another criterion for establishing L_R.

In the current work, the apparent thermal resistivities were calculated from the total heat flux through the specimens,

$$R_L^a = \frac{\Delta T}{q_t} = \frac{R}{L} \quad . \tag{73}$$

Thus, these resulting values equal the average or mean thermal resistivities. Rearrangement of Eq. (73) yields

$$R = R_L^a L \quad , \tag{74}$$

and combination of Eq. (74) with Eq. (35) or (49) yields

$$R = A(E)L + \frac{B(E)}{E} \quad . \tag{75}$$

The values of $A(E)$ and $B(E)$ have been determined for $\tau^\circ > 2$ and are given in Table 10.

Substituting Eq. (75) into Eq. (71) or (72) shows that the differential thermal resistivity is equal to $A(E)$, a constant, for a material with a fixed extinction coefficient and for $\tau^\circ > 2$. Since $A(E)$ is the

same for $\omega = 0$ or 1, the differential thermal resistivity has the same value for a given material whether thermal photons are scattered, absorbed, or both. Since $A(E)$ equals $1/k_{eff}$, the differential thermal resistivity equals

$$R_L = \frac{1}{k_c + (16n^2\bar{\sigma}\bar{T}_m^3)/3E} \tag{76}$$

for $\tau^\circ > 2$ and any albedo.

The ASTM method for determining L_R requires the determination of the thickness at which the value of the differential thermal resistivity is within 2% of the value for the mean thermal resistivity of the biggest sample that is to be characterized or that could be tested. As the differential value is a constant for a given material for $\tau^\circ > 2$ and as the mean value will be decreasing as L increases, the ASTM method establishes the minimum thickness for an insulation above which the definition of the thermal conductivity applies. For products with full-use thickness less than L_R, testing should be done at conditions applicable to their use.

The representative thickness, $\bar{L}_R$, as defined by ASTM C177-76 is the value of L for which the mean thermal resistivity [Eq. (35) or (49)] is 1.02 times the differential thermal resistivity, Eq. (76),

$$A(E) + \frac{B(E)}{E\bar{L}_R} = 1.02A(E) \ , \tag{77}$$

or

$$L_R = 50\,\frac{B(E)}{EA(E)} \ . \tag{78}$$

The representative thickness L_R is given by

$$L_R = \frac{600B(\alpha)k_{eff}}{\alpha} \tag{79}$$

for the pure absorption case, and

$$L_R = \frac{12\left[\frac{4}{3}\left(\frac{2}{\varepsilon} - 2\right) + \gamma\right]\left(\frac{50k_s}{k_{eff}} - \frac{k_c}{k_{eff}}\right)}{\sigma} \tag{80}$$

for the pure scattering case, where α and σ are in ft^{-1} and L_R is in inches. Equation (80) is in agreement with Rennex.[7] Representative thicknesses for specimens having extinction coefficients between 10 and 100 ft^{-1} are given in Table 12.

The value for $B(E)$ with $\omega = 0$ and $\varepsilon = 1$ [i.e., $B(\alpha)$] was the lower limit for $B(E)$ at a given value of E. The value of $B(E)$ with $\omega = 1$ and $\varepsilon \neq 1$ [i.e., $B(\sigma)$] was the upper limit. Since $A(E)$ is independent of ω and ε the values of L_R given in Table 12 represent the upper and lower limits of the representative thickness as set forth by the ASTM specification. If the extinction coefficient is in the range 50 to 150 ft^{-1} as calculated from Pelanne's data,[16] then the representative thickness is in the range 1.27 in. (E = 150, ω = 0, ε = 1) to 13.3 in. (E = 50, ω =1, ε = 0.9). If an average E of 100 ft^{-1} is assumed typical, then L_R

Table 12. Representative Thicknesses for Guarded Hot-Plate Test Specimens

E (ft^{-1})	Representative Thickness, in.		
	$\omega = 0$, $\varepsilon = 1$	$\omega = 1$, $\varepsilon = 1$	$\omega = 1$, $\varepsilon = 0.9$
10	61.1	76.9	92.9
25	19.0	26.8	32.3
50	7.19	11.0	13.3
75	3.93	6.21	7.50
100	2.44	4.03	4.87
125	1.71	2.84	3.43
150	1.27	2.11	2.55
200	0.78	1.30	1.57
500	0.15	0.24	0.29
1000	0.037	0.057	0.069

varies from 2.44 in. ($\omega = 0$, $\varepsilon = 1$) to 4.87 in. ($\omega = 1$, $\varepsilon = 0.9$). This large range of L_R values indicates the importance of the characteristics of the apparatus and the insulation optical properties.

Equations (35) and (49) show that the apparent (mean) thermal resistivity continues to decrease until L reaches infinity. Thus, an alternate definition of L_R could be the thickness at which the thermal resistivity equals 1.02 times the value at infinite thickness. The criterion based on the mean thermal resistivity is

$$A(E) + \frac{B(E)}{EL_R} = 1.02\left[A(E) + \frac{B(E)}{E\infty}\right] = 1.02A(E) \quad . \tag{81}$$

As Eqs. (77) and (81) are identical, the ASTM method and this alternate method based on the mean thermal resistivity are identical. As noted above, above this L_R the ASTM definition of thermal conductivity applies. For products with full-use thickness $L_F < L_R$, this criterion leads to the following expression for L_R:

$$L_R = \frac{50B(E)/EA(E)}{1 + \left[51B(E)\right]\left[EA(E)L_F\right]} \quad . \tag{82}$$

A third method for fixing L_R is to use the differential thermal resistivity. This procedure would require the determination of the thickness above which the differential thermal resistivity would not change by more than 2% with further increases in thickness. The analyses performed earlier in this section and in Sect. 5.2, however, show that the value of $A(E)$ and, hence the differential thermal resistivity, does not change for $\tau^\circ > 2$. Therefore, this third method would be independent of ω and ε and fix L_R as

$$L_R \leq \frac{2}{E} \quad . \tag{83}$$

Based on this criterion, for E equal to 50, 100 or 150 ft^{-1}, L_R equals 0.48, 0.24, or 0.18 in., respectively.

If the third method for determining L_R is used, the full-thickness resistance of the material can be determined from two or more measurements of the thermal resistance of the material at thicknesses greater than L_R. The measurements are then used to empirically establish the linear relationship between R and L. Table 13 shows the ratios of the resistance obtained from either the numerical or three-region solution to the value calculated from a one-parameter line based upon a measurement on a 1-in.-thick sample, where

$$R = R_L^{\alpha}(1 \text{ in.})L \quad . \tag{84}$$

The values from Eq. (84) show errors as large as 17.8% (α = 50 ft^{-1}, ω = 1, and L = 12 in.). They are within 2% of the numerical solution's R-value for L less than 2 in. and E less than 150 ft^{-1} or 3.5 in. for E = 200 ft^{-1}.

Table 14 shows the ratio of the solution resistance to that calculated from a least squares line obtained from the values of R calculated at 0.042 (1/2 in.), 0.083 (1 in.), and 0.1667 ft (2 in.). Table 14 shows that the resulting R-values from the two-parameter fit are within 2% of the value obtained by the numerical or three-region solutions.

The above observations have been further tested using R-value data recently published by Tye et al.[21] The data include R-values for a range of specimen thicknesses from 1.44 to 7.22 in. The R-values at specific insulation densities were calculated from measurements of apparent thermal conductivity and a correlation of apparent thermal conductivity and density. Apparent thermal conductivities were determined to within 3% from full-thickness guarded hot-plate measurements. An analysis was made using sets of measured R-values of fiberglass insulation from three manufacturers. The R-value data for a given manufacturer's product were divided into groups having density ranges of 0.1 lb/ft^3. For example, R-value data at various thicknesses with densities in the interval from 0.55 to 0.65 lb/ft^3 were grouped for the analysis. Finally, each group of R-values was adjusted to constant density using an empirical expression

Table 13. Ratio of Thermal Resistance from Eq. (75) to the Value from Eq. (84)

Thickness (in.)	Ratio for Various E at			
	50 ft^{-1}	100 ft^{-1}	150 ft^{-1}	200 ft^{-1}
	$\omega = 0, \varepsilon = 1$			
1	1.0	1.0	1.0	1.0
2	1.067	1.024	1.013	1.008
3.5	1.099	1.034	1.018	1.011
6	1.117	1.040	1.021	1.013
9	1.126	1.043	1.022	1.014
12	1.130	1.045	1.023	1.014
	$\omega = 1, \varepsilon = 1$			
1	1.0	1.0	1.0	1.0
2	1.090	1.036	1.020	1.013
3.5	1.133	1.053	1.029	1.018
6	1.159	1.062	1.034	1.021
9	1.172	1.066	1.036	1.023
12	1.178	1.068	1.037	1.023

Table 14. Ratio of R from Eq. (75) to R Obtained from a Two-Parameter Line Fit to Data at 0.5, 1, and 2 in.

Thickness (in.)	Ratio for Various E at			
	50 ft^{-1}	100 ft^{-1}	150 ft^{-1}	200 ft^{-1}
	$\omega = 0, \varepsilon = 1$			
1	1.00085	0.99991	1.00021	1.00007
2	0.99985	1.00001	0.99997	0.99999
3.5	0.99965	1.00008	1.00035	1.00028
6	0.99995	1.00068	1.00042	1.00035
9	0.99962	1.00068	1.00045	1.00039
12	1.00064	1.00069	1.00047	1.00041
	$\omega = 1, \varepsilon = 1$			
1	1.00485	1.00163	1.00075	1.00041
2	0.99652	0.99988	0.99949	0.99973
3.5	0.98948	0.99672	0.99853	0.99921
6	0.98448	0.99523	0.99788	0.99887
9	0.98184	0.99447	0.99754	0.99869
12	0.98045	0.99406	0.99737	0.99860

for thermal conductivity versus density that was reported by Tye et al.[21] Seven sets of R-values at constant density and given manufacturer were so generated.

The seven sets of data were used to test the applicability of Eq. (75) for describing the R-value data and to compare Eq. (75) with Eq. (84). For each set of data the constants in the two equations were computed using the method of least squares and the variances were calculated. As expected, the variances obtained using Eq (75) were always less than those obtained using Eq. (84). The differences between the two equations were not dramatic. The results, however, which are summarized in Table 15, are fully supportive of Eq. (75).

A more revealing test of the applicability of Eq. (75) was provided by four sets of data of R-values on approximately 1.5 in., 3 in., and full-thickness specimens. The approach was to calculate a value for R at full thickness using both Eq. (84) with the constant determined from a thin specimen and Eq. (75) with the slope $\Delta R/\Delta L$ determined from two thin-specimen R-value measurements. The calculated R-values at full thickness are compared with the experimental values in Table 16. The results in the table clearly show an improvement resulting from the use of Eq. (75) to obtain full-thickness R-values.

Table 15. Summary of Results Obtained Using Eqs. (75) and (84) to Describe Experimentally Determined R-Values

Manufacturer	Density (lb/ft^3)	Number in Data Set	Eq. (84) Slope	Eq. (75)		Eq. (84) Variance[a]	Eq. (75) Variance
				Slope	Intercept		
A	0.5	8	2.699	2.607	0.3904	0.088	0.076
A	0.6	8	2.801	2.616	0.8649	0.689	0.633
A	0.7	8	3.065	2.955	0.5990	0.461	0.432
B	0.4	19	2.616	2.383	1.179	0.635	0.555
C	0.5	10	2.841	2.568	1.035	0.686	0.628
C	0.6	19	2.994	2.968	0.124	0.303	0.300
C	0.7	18	3.141	3.031	0.508	0.131	0.061

[a] $\sum_{i=1}^{n}\left[R_i(\text{exp}) - R_i(\text{calc})\right]^2/(n-s)$, where n = number of points in the data set and s = 1 for Eq. (84) and 2 for Eq. (75).

Table 16. Comparisons of Full-Thickness R-Values from Eqs. (75) and (84) with Experimental Results

Method Used to Obtain Full Thickness R-Value	R-Values for each Data Set[a]				
	A (1204-3)	B (1205-3)	C (1206-3)	D (1206-4)	Average
Eq. (84) with data at thickness of 1.44 in.[b]	18.79	18.75	17.39	18.49	18.4
Deviation from experimental value, %	4.6	10.3	9.8	5.5	7.6
Eq. (75) with data at thickness of 1.44 and 2.88 in.	18.48	16.25	16.36	17.59	17.17
Deviation from experimental value, %	2.9	−4.4	3.3	0.4	2.8[c]
Full-thickness measurement	17.96	17.00	15.84	17.52	17.08
Full-thickness, in.	6.00	6.00	5.10	5.64	

[a]Data from ref. 21 are for measurements on quadrasected nominal 6 in. fiberglass batts coded in the reference with the numbers in parentheses.

[b]Exact thicknesses are given in ref. 21.

[c]Average of the absolute deviations.

6. CONCLUSIONS

The most significant accomplishments and conclusions are enumerated below.

1. A numerical procedure was developed and applied to solve the coupled conductive and radiative heat transfer problem of an infinite slab of an absorbing and emitting gray medium bounded by black plates. This procedure allowed an assessment of the effects of boundary conditions and media properties on the apparent thermal properties of the media.

2. The accuracy of the total heat flux obtained from the numerical procedure was established as 0.1% of the calculated value. This accuracy was determined by comparing the numerical solution results with the heat fluxes obtained from the optically thin and thick analytical solutions and with alternate solutions found in the literature.[1,2]

3. The numerical solution was used to model measurement of the apparent thermal conductivity of insulation for specimens with optical thickness less than 40. Calculations were performed for absorption coefficients between 0.001 and 1000 ft^{-1} and specimen thicknesses between 0.0208 and 1.0 ft.

4. A three-region approximation to the coupled heat transfer problem was developed and shown to yield results within ±0.5% of the apparent thermal conductivity obtained from the numerical technique for optical thicknesses greater than 4.

5. The three-region approximate solution to the coupled problem ($\omega = 0$) and the numerical solution to the uncoupled problem ($\omega = 1$) were used to show that

$$\frac{1}{k_{app}} = \frac{1}{k_{eff}} + \frac{B(E)}{\tau^{\circ}} \tag{85}$$

The values of $B(E)$ were determined for the limiting cases of pure absorption ($\omega = 0$) and pure scattering ($\omega = 1$).

6. Data available in the literature[1] were used to show that the plate emissivity had an effect on $B(E)$ and that the value of $B(E)$ for the pure absorption case with black plates fixed a lower limit for $B(E)$, while the value obtained for the pure scattering case with nonblack plates fixed the upper limit.

7. The apparent thermal conductivity for the pure absorption and pure scattering cases were shown to depend on T_m, where $T_m = [(T_1^2 + T_2^2)(T_1 + T_2)/4]^{1/3}$.

8. A small change in the continuous-phase thermal conductivity resulting from solid-phase conduction or convection produces the same change in the apparent thermal conductivity.

9. The results of the analysis provide a method to establish how critical parameters define the range of apparent thermal conductivity of building insulations, for example, representative sample thicknesses.

10. An analysis of existing data for fiberglass batts supports the use of Eq. (75) for the correlation of R-values with specimen thicknesses above 1 in. The slope in Eq. (75) can be used to determine full-thickness R-values from thin specimen measurements more accurately than Eq. (84).

7. RECOMMENDATIONS

The three-region approximation and the numerical solution are valuable tools for the analysis of coupled conductive and radiative heat transfer in an absorbing and emitting slab bounded by black surfaces. The usefulness of these solutions can, however, be greatly increased by extending the analyses to include varying emissivity and albedo. With these analyses completed, it may be possible to determine the properties of insulation, such as extinction coefficient and albedo, by making apparent thermal conductivity determinations at several mean test temperatures. Furthermore, once the extinction coefficient and albedo are determined, the effects of sample thickness and plate emissivity will also be established. Thus, one set of experiments may lead to a thorough understanding of the relationship between sample properties and test conditions for all similar types of insulation.

Further development of theoretical analyses must incorporate accurate experimental data, which should be obtained on well-characterized specimens. The aim of this program should be the validation of the theoretical analyses through accurate measurement of apparent thermal conductivity as a function of thickness, temperature, emissivity, and continuous-phase thermal conductivity. Development of techniques for extinction coefficient and albedo measurments on insulation must also be part of the experimental program.

Since insulation is often used in shapes that have cylindrical or spherical symmetry, analyses of heat transfer in cylindrical and spherical coordinates should be undertaken to develop an understanding of how the properties of insulation are affected by these geometries and how the results of measurements on planar samples must be corrected when the insulation is used in another shape.

Finally, an effort should be made to use Eq. (75) for the determination of full-thickness R-values from measurements on relatively thin specimens. The Eq. (75) extrapolation of measured R-values to full-thickness R-values when combined with improvements in determining R-value density dependence should be considered in the development of improved standards for measurement.

8. REFERENCES

1. R. Viskanta, "Heat Transfer by Conduction and Radiation in Absorbing and Scattering Materials," *J. Heat Transfer* 87C: 143 (1965).
2. C. C. Lii and N. Ozisik, "Transient Radiation and Conduction in an Absorbing, Emitting, Scattering Slab with Reflective Boundaries," *Int. J. Heat Mass Transfer* 15: 1175 (1972).
3. "ASTM C 177-76," pp. 19–52 in *1979 Annual Book of ASTM Standards,* Pt. 18, American Society for Testing and Materials, Philadelphia, 1979.
4. "C-16 Statement on Thermal Resistance of Thick, Low Density Insulations (Oct. 25, 1978)," *ASTM Standardization News,* 7(3): 37 (1979).
5. "Trade Regulations: Labeling and Advertising of Home Insulation," *Fed. Regist.* 44(167): 50218–45 (1979).
6. "Residential Conservation Service Program," *Fed. Regist.* 44(217): 64602–727 (1979).
7. B. G. Rennex, "Thermal Parameters as a Function of Thickness for Combined Radiation and Conduction Heat Transfer in Low-Density Insulation," *Journal of Thermal Insulation,* in press.
8. T. T. Jones, "The Effect of Thickness and Temperature on Heat Transfer Through Foamed Polymers," pp. 737–48 in *Thermal Conductivity, Proc. 7th Conf.,* NBS Spec. Publ. 302, 1968.
9. R. B. Bhattacharyya, "Heat Transfer Model for Fibrous Insulation," presented at the DOE/ASTM Thermal Insulation Conference, Tampa, Fla., October 1978.
10. R. Viskanta and R. J. Grosh, "Heat Transfer by Simultaneous Conduction and Radiation in an Absorbing Medium," *J. Heat Transfer* 84C: 63 (1965).
11. R. Viskanta, "Heat Transfer in Thermal Radiation-Absorbing and Scattering Media," ANL-6170, (1960).
12. E. M. Sparrow and R. D. Cess, *Radiation Heat Transfer,* Brooks/Cole Publishing Co., Belmont, Calif., 1970.

13. R. Siegel and J. R. Howell, *Thermal Radiation Heat Transfer,* McGraw-Hill, New York, 1972.

14. M. A. Heaslet and R. F. Warming, "Radiative Transport and Wall Temperature Slip in an Absorbing Planar Medium," *Int. J. Heat Mass Transfer* 8: 979 (1965).

15. W. Lick, "Energy Transfer by Radiation and Conduction," p. 14 in *Proc. 1963 Heat Transfer and Fluid Mechanics Institute,* Stanford University Press, Palo Alto, Calif., 1973.

16. C. M. Pelanne, "Light Transmission Measurements Through Glass Fiber Insulation," p. 263 in *Proc. ASTM C-16 Committee Symp. Thermal Transmission Measurements of Insulation,* ASTM Spec. Tech. Publ. 660 American Society for Testing and Materials, Philadelphia, 1978.

17. A. Euken, *Thermal Conductivity of Ceramic Refractory Materials. Its Calculation from the Thermal Conductivity of Constituents,* VDI-Verlag, Berlin, 1932. Abstracted in *Ceram. Abstr.* 11(11): 576 (1932).

18. M. Abramowitz and I. A. Stegun, Eds., *Handbook of Mathematical Functions,* National Bureau of Standards, Washington, D.C., 1965, p. 227.

19. R. Viskanta and R. J. Grosh, "Effect of Surface Emissivity on Heat Transfer by Simultaneous Conduction and Radiation," *Int. J. Heat Mass Transfer* 5: 729 (1962).

20. Private communication, B. G. Rennex, National Bureau of Standards, Washington, D.C., to H. A. Fine, University of Kentucky, Lexington, June 1980.

21. R. P. Tye, A. O. Desjarlais, D. W. Yarbrough, and D. L. McElroy, *An Experimental Study of Thermal Resistance Values (R-Values) of Low-Density Mineral-Fiber Building Insulation Batts Commercially Available in 1977,* ORNL/TM-7266 (April 1980).

APPENDIX A

DEFINITIONS AND TECHNIQUE FOR MEASUREMENT OF THERMAL PROPERTIES*

4. TERMINOLOGY

Note 9 — As Definition C168 is under revision, the definitions and symbols given here should be used.

4.1 Definitions

4.1.1 Thermal Resistance, R

The temperature difference required to produce a unit of heat flux through the specimens under steady-state conditions. For a flat slab, it is calculated as follows:

$$R = \frac{A(T_1 - T_2)}{Q} = \frac{1}{\Gamma} = \frac{D}{\lambda}$$

4.1.2 Thermal Conductance, Γ

Under steady-state conditions, the heat flux required to produce a unit temperature difference; the reciprocal of the thermal resistance of the specimen. For a flat slab, it is calculated as follows:

$$\Gamma = \frac{Q}{A(T_1 - T_2)} = \frac{1}{R} = \frac{\lambda}{D}$$

4.1.3 Thermal Conductivity, λ

Under steady-state conditions, the heat flux per unit temperature gradient in the direction perpendicular to an isothermal surface. For thin specimens or low-density materials this definition must be applied

---

*Reprinted from ASTM C177-76, *Standard Test Method for Steady-State Thermal Transmision Properties by Means of the Guarded Hot Plate,* with the permission of the American Society for Testing and Materials (ASTM). This standard may be obtained from ASTM, 1916 Race St., Philadelphia, Pennsylvania 19103.

with caution. Thermal conductivity of a material can be defined only where several conditions are met (see 1.6): the thermal resistance of specimens of a material must be sufficiently independent of the area of the specimen, of where the specimen is selected in the sample, of the temperature difference across the specimen, and, for a flat slab specimen, the thermal resistance must be proportional to the thickness. The latter can be demonstrated by plotting the thermal resistance of a number of specimens of the material against specimen thickness. The line through the point must increase linearly with thickness from zero thermal resistance at zero thickness. When this condition is met, the thermal conductivity can be determined as the inverse of the slope of the straight line and the thermal conductivity can be calculated as follows:

$$\lambda = \frac{Q \times D}{A(T_1 - T_2)} = \frac{D}{R}$$

The above requirement assumes that the heat transfer within the specimen is independent of thickness and temperature difference. It recognizes the existence of a minimum thickness and maximum temperature difference for which thermal conductivity can be defined. For the purposes of this method, a 2% dependence will be considered maximum for each.

4.1.4 Thermal Resistivity, r

Under steady-state conditions, the temperature gradient, in the direction perpendicular to the isothermal surface, per unit heat flux; the reciprocal of the thermal conductivity. It can only be defined when thermal conductivity can be defined. For a flat slab, it is calculated as follows:

$$r = \frac{A(T_1 - T_2)}{Q \times D} = \frac{1}{\lambda} = \frac{R}{D}$$

4.2 Symbols

The symbols used in this method have the following significance (Note 10):

λ = thermal conductivity, $W \cdot m^{-1} \cdot K^{-1}$ or $W \cdot m \cdot K^{-1} \cdot m^{-2}$

r = thermal resistivity, $K \cdot m \cdot W^{-1}$ or $K \cdot m^2 \cdot W^{-1} \cdot m^{-1}$

Γ = thermal conductance, $W \cdot m^{-2} \cdot K^{-1}$

R = thermal resistance, $K \cdot m^2 \cdot W^{-1}$

Q = time rate of heat flow, W

q = heat flux, that is, time rate, of heat flow per unit area, $W \cdot m^{-2}$

A = area measured on a selected isothermal surface, m^2

D = thickness of specimen measured along a path normal to isothermal surfaces, m

T_1 = temperature of warm surface of specimens, K or °C

T_2 = temperature of cold surface of specimens, K or °C

Note 10 — Various units may be found for the thermal properties in the literature. The International System of Units is used exclusively in this test method and conversion factors to inch-pound and kilogram-calorie systems can be found in Tables 2a and 2b for thermal resistance and thermal conductivity.

X1.4 Determining the Thermal Conductivity and Resistivity of a Material

X1.4.1 General — A thermal property of a material can be determined by a single measurement only if the sample is typical of the material, and the specimen(s) are typical of the sample. The procedure for selecting the sample should normally be specified in the material specification, or directly by the parties concerned. The selection of the specimen from the sample can be partly specified in the material specification and partly in the test method. The specification in the test method must be given priority and disregarded only after careful technical consideration. A number of these requirements have been given above. The thermal resistance of a material is known to depend on the relative magnitudes of the heat transfer process involved. Thermal conduction, radiation, and

convection are the primary mechanisms. Of these, only conduction is linearly dependent on ΔT. These processes are well researched, but they can combine, or couple, to produce nonlinear effects that are difficult to analyze, and even more difficult to measure.

X1.4.2 Dependence of Specimen Thickness — Of the process involved, only conduction produces a heat flow that is directly proportional to the thickness of a specimen. The others result in a more complex relationship. The thinner and less dense the material, the more likely that the resistance depends on processes other than conduction. The result is a condition that does not satisfy the requirements of the definitions for thermal conductivity and thermal resistivity, both defining intrinsic properties, since the apparent respective values show a dependence on the specimen thickness. For such materials, it may be desirable to determine the thermal resistance at conditions applicable to their use. There is believed to be a lower limiting thickness for all materials below which such a dependence occurs. Below this thickness, the specimen may have unique thermal transmission properties, but not the material. It remains, therefore, to establish this minimum thickness by measurements.

X1.4.3 Dependent on Temperature Difference — The magnitude of all the thermal transfer processes depends on the temperature difference across the specimen. The dependence is more complex than direct proportionality for all processes except conduction. For many materials the complex dependence occurs at temperature differences that are typical of use. In such a case, it is wise to use a value for the test that is typical of use, and to determine an approximate relationship for a range of temperature differences. The dependence can be linear for a wide range in temperature differences.

X1.4.4 Method of Determining Dependence on Temperature Difference — If the temperature-difference dependence of the thermal properties is not known for a material, a minimum of three measurements is necessary. These are made with widely differing temperature differences. A second-order dependence can be revealed by these measurements. When a simple linear relationship is known to occur, only two measurements, that is, one extra, need be made. This establishes the linear dependence for that particular sample.

X1.4.5 Determination of Minimum Thickness for Which Thermal Properties of the Material May Be Defined — If the minimum thickness for which the thermal conductivity and resistivity can be defined is not known, it is necessary to estimate this thickness. There is no established procedure for determining this thickness (Note X1). The somewhat crude procedure outlined below may be used for determining the thickness and whether it occurs in the range of thickness in which a material is likely to be used (Note X3).

Note X1 — If improved methods for determining the thickness in question are developed or proposed, ASTM Subcommittee C16.30 would appreciate receiving information about them. Contact the chairman of the subcommittee through ASTM Headquarters.

X1.4.6 Procedure:

X1.4.6.1 Select a uniform sample of material of thickness equal to the greatest thickness to be characterized, or to the maximum allowable thickness for the test apparatus. This thickness is termed D5.

Note X2 — This particular test may be conducted in the Guarded Hot Box, Method C236.

X1.4.6.2 Cut five sets of specimens from the samples. These should range in thickness from the smallest thickness likely to be used in practice, termed D1, to D5 in approximately equal increments. The sets of specimens are then designated S1 to S5 according to their thickness.

X1.4.6.3 Measure the thickness and thermal resistances of S1, S3, and S5.

X1.4.6.4 Calculate (R3-R1)/(D3-D1), (R5-R3)/(D5-D3), and R5/D5. These are termed $\Delta R/\Delta D$ values.

X1.4.6.5 If these three values differ by less than 2%, then the material can be characterized by a thermal conductivity and resistivity.

X1.4.6.6 If the three values differ by more than 2%, then measure the thickness and thermal resistance of S2 and S4. Calculate the values of (R2-R1)/(D2-D1), (R3-R2)/(D3-D2), (R4-R3)/(D4-D3), (R5-R4)/(D5-D4) and R5/D5.

Note X3 — It is important to differentiate between added thermal resistance in measurements caused by the placement of the thermocouples below the surfaces of the plates, added resistance caused by poor specimen surfaces, and added thermal resistance caused by the coupling of the conduction and radiation modes of heat transfer in the specimens. All three can affect the measurements in the same way, and often the three may be additive.

X1.4.6.7 Thicknesses above which all the $\Delta R/\Delta D$ values agree with the value of R5/D5 to within 2% may be characterized by thermal conductivity and thermal resistivity. Allowance must be made in interpretation of the results for experimental error. A plot of the $\Delta R/\Delta D$'s and R5/D5 versus thickness may aid in reducing the uncertainty. Least squares curve fitting of R versus D may also help. A larger number of specimens may be used where greater definition is required. Thickness dependence may be a function of mean temperature and temperature difference across the specimens. For the purposes of this method, this single check, if performed at typical operating temperature and temperature differences, shall be adequate to indicate the degree of thickness dependence.

APPENDIX B

PDP/8e FOCAL PROGRAM LISTING, TYPICAL OUTPUT AND NOMENCLATURE LIST FOR THE NUMERICAL SOLUTION

```
C-FOCAL.J4.CODASIII  33534W

01.01 C RADIATION/CONDUCTION IN SLAB. FILE 3. SHJ 1 AUG 79
01.02 L S 3,4;G 14.01
01.60 F I=0,N;D 2
01.70 F J=0,N;D 9
01.75 S A=0;F J=1,N;S A=A+(FSTR(9500+J)+FSTR(9500+J-1))*AL*L/(2*N)
01.80 S Q=CA*(TH-TC)/L+2*SI*TC↑4*(FSTR(3500+N)-1/3)/(AL*L)
01.85 S Q=Q+2*SI*TH↑4*(-FSTR(3500+N)/(AL*L)-1/2+1/(3*AL*L))+SI*TH↑4
01.86 S Q=Q+2*SI*A
01.90 T !!;T "A=",%,A," Q=",Q," K EFF=",%8.06,Q*L/(TH-TC),!!!
01.96 G 15.21

02.05 S TL=TC/TH+(I/N)*(1-TC/TH)
02.07 S T2=FSTR(9000+I)
02.09 S DF=T2-TL;S T3=T2*TH;S T4=T3-TC-(TH-TC)*I/N
02.11 T %3,I,%8.06,T2,DF,%10.03,T3,T4,!

09.01 C EVALUATION OF Q
09.02 S NK=N-J;S D1=FSTR(3000+NK)-FSTR(3000+J)
09.05 S EG=(RI↑2/(L*AL))*D1*(FSTR(9000+J)*TH)↑4
09.06 S DU=FSTR(9500+J,EG);R

15.01 C-MULTIPLE INPUT
15.06 A "NO. OF CALCS. TO ENTER=",NO,!;T "ENTER AL,K,L,TC,TH,RI,",!
15.16 F II=1,NO;A AL(II),CA(II),L(II),TC(II),TH(II),RI(II),!
15.19 S II=1
15.21 I (NO-II) 15.99,15.26
15.26 S AL=AL(II);S CA=CA(II);S L=L(II);S TC=TC(II);S TH=TH(II)
15.27 S N=FITR(AL*L/(5*.12)+.5);S N=5*N
15.28 I (N-50)15.3;I (N-495)15.31;S N=495;G 15.31
15.30 S N=50
15.31 S RI=RI(II);S II=II+1;S SI=.1714E-8
15.32 S RC=CA*AL/(4*SI*TH↑3);S DU=FSTR(9000,TC/TH);S DU=FSTR(9000+N,1)
15.33 S IV=10000;S DU=FSTR(IV+1,AL);S DU=FSTR(IV+2,CA);S DU=FSTR(IV+3,L)
15.34 S DU=FSTR(IV+4,TC);S DU=FSTR(IV+5,TH);S DU=FSTR(IV+6,RI)
15.35 S DU=FSTR(IV+7,N);S DU=FSTR(IV+9,SI);S DU=FSTR(IV+11,RC)
15.40 T !!,"CASE NO.=",%3,II-1,!!;T "AL=",%12.04,AL,!
15.42 T "CA=",%10.06,CA," L=",L," RC=",RC,!
15.45 T " TC=",%6,TC," TH=",TH," RI=",RI," N=",N
15.46 L S 3,9;G 11.02
15.50 L P 3
15.60 T "TIME,HR=",%6.02,FTIM(0)/3600,!;L S 3,4;G 1.11
15.99 Q
*
```

```
C-FOCAL.J4.CODASIII 33534W

01.01 C RADIATION/CONDUCTION IN SLAB. FILE 4. SHJ 16 JULY 79
01.02 D 1.36; L S 4,9; G 1.51
01.11 S IV=10000; S AL=FSTR(IV+1); S CA=FSTR(IV+2); S L=FSTR(IV+3)
01.12 S TC=FSTR(IV+4); S TH=FSTR(IV+5); S RI=FSTR(IV+6)
01.13 S N=FSTR(IV+7); S SI=FSTR(IV+9); S RC=FSTR(IV+11)
01.32 S W1=AL*L; D 12; S DU=(TC/TH)↑4
01.33 S BE=1+(1-DU)*(1/3-E4)/(10*2*RC*(1-TC/TH))
01.34 S XS=1-.5*FSQT(TC/TH)/((1+FSQT(W1))*(1+10*RC))
01.36 F I=0,N; D 3.1; S DU=FSTR(4500+I,(TC+(D+1)*I*(TH-TC)/(N+D*I))/TH)
01.40 T "XS=",%7.03,XS," BETA=",BE,!!; F I=0,N; S W1=AL*I*L/N; D 2
01.45 F I=0,N; D 4; S DU=FSTR(4000+I,G)
01.98 L P 4
01.99 L S 4,9; G 1.11

02.01 C EVALUATION OF E INTEGRALS
02.05 S E3=0; S E4=0; I (2.33998+W1)2.15,2.15; I (10-W1)'2.07; D 12
02.07 S DU=FSTR(3500+I,E4)
02.15 S DU=FSTR(3000+I,E3); R

03.10 S D=(BE-1)*(1-I/(N*XS)); R

04.01 C CALCULATION OF G(I)
04.05 S G=(1/(2*RC))*(TC/TH)↑4
04.07 S G=G*(-FSTR(3500+I)+I*FSTR(3500+N)/N+(1-I/N)/3)
04.10 S G1=((1-I/N)*FSTR(3500+N)-FSTR(3500+N-I)+I/(3*N))/(2*RC)
04.20 S G=G+G1+(TC/TH+(I/N)*(1-TC/TH)); R

12.01 C EVALUATION OF E3 INTEGRAL
12.05 I (W1)12.50,12.45,12.1
12.10 I (W1-1)12.15,12.15,12.30
12.15 S E1=A0-FLOG(W1)+A1*W1+A2*W1↑2+A3*W1↑3+A4*W1↑4+A5*W1↑5; GO TO 12.35
12.30 S E1=(W1↑4+B1*W1↑3+B2*W1↑2+B3*W1+B4)
12.31 S E1=E1/((W1↑4+C1*W1↑3+C2*W1↑2+C3*W1+C4)*(W1*FEXP(W1)))
12.35 S E2=FEXP(-W1)-W1*E1
12.40 S E3=(FEXP(-W1)-W1*E2)/2; D 13; R
12.45 S E3=.5; S E4=1/3; R
12.50 S W1=-W1; S EI=.57721566+FLOG(W1); S S1=1; S KK=0; S KA=1
12.60 S KK=KK+1; S KA=KA*KK; S S1=S1*W1
12.65 S EI=EI+S1/(KK*KA)
12.70 I (1E-6-FABS(S1/(KK*KA*EI)))12.6
12.80 S E3=((1+W1)*FEXP(W1)-W1↑2*EI)/2; R

13.01 C EVALUATION OF E4 INTEGRALS
13.10 S E4=(FEXP(-W1)-W1*E3)/3; R

14.01 C ENTER PARAMETER VALUES
14.05 S A0=-.57721566; S A1=.99999193; S A2=-.24991055; S A3=.05519968
14.10 S A4=-.00976004; S A5=.00107857; S B1=8.57332874; S B2=18.05901697
14.15 S B3=8.63476089; S B4=.26777373; S C1=9.57332235
14.20 S C2=25.63295615; S C3=21.09965308; S C4=3.95849693; L P 4
14.21 L S 4,3; G 15.01
*
```

```
C-FOCAL.J4.CODASIII  33534W

01.01 C RADIATION/CONDUCTION IN SLAB.  FILE 9.  SHJ  1 AUG 79
01.02 T "Z=",%,Z,"    TIME,HR.=",%6.02,FTIM(0)/3600,!;R
01.11 S IV=10000;S AL=FSTR(IV+1);S CA=FSTR(IV+2);S L=FSTR(IV+3)
01.12 S TC=FSTR(IV+4);S TH=FSTR(IV+5);S RI=FSTR(IV+6)
01.13 S N=FSTR(IV+7);S SI=FSTR(IV+9);S RC=FSTR(IV+11)
01.14 S JJ=10*N/(AL*L);L P 9
01.51 F I=1,N-1;D 7;S T2=FSTR(4000+I)+A/(2*RC);S DU=FSTR(9000+I,T2)
01.52 S Z=0;S DU=FSTR(9001)-(TC/TH+(1-TC/TH)/N);F I=0,N;D 10
01.53 I (2-Z)1.97;D 1.02;I (DU+1E-4)1.54;I (Z-1E-4)1.59,1.55,1.55
01.54 T "BETA=",%7.03,N*(TH*FSTR(9001)-TC)/(TH-TC),!
01.55 F I=0,N;D 1.58
01.57 GOTO 1.51
01.58 S T1=(FSTR(9000+I)+M*FSTR(4500+I))/(M+1);S DU=FSTR(4500+I,T1)
01.59 T %,"A=",A,!!!,"    I        F2        F2-FL            TCALC    TCALC-TLIN
01.60 T,!!
01.70 L S 9,3;G 1.6
01.97 S M=1+2*M;T !,"LARGE ERROR=",%,Z,"    REPEAT USING M=",%4,M,!!
01.98 L S 9,4;G 1.02

07.01 C EVALUATION OF T2(I) INTEGRAL
07.05 S IN=0;S A=0;F J=0,N;D 8
07.99 R

08.01 C ADJUNCT TO GROUP 7
08.02 S DU=0;I (JJ-J)8.05;S DU=FSTR(3000+J)
08.05 S D1=0;S K=FABS(I-J);I (JJ-K)8.07;S D1=FSTR(3000+K)
08.07 S D2=0;S NK=N-J;I (JJ-NK)8.09;S D2=FSTR(3000+NK)
08.09 S D1=-D1+DU;S D2=D2-DU
08.10 S EF=RI*2*(D1+D2*I/N)*FSTR(4500+J)*4;I (-IN)8.2;D 9;R
08.20 S A=A+(U+EF)*AL*L/(2*N)
08.30 D 9.1;S IN=1;R

09.01 C ADJUNCT TO GROUP 8
09.05 S IN=IN+1
09.10 S U=EF;R

10.01 C LARGEST ERROR DETECTOR
10.04 I (I-1)10.99;S ER=FABS(1-FSTR(9000+I)/FSTR(4500+I))
10.10 I (ER-Z)10.99;S Z=ER
10.99 R

11.01 C SET START VALUE OF M
11.02 S M=1;T "  M=",%6,M,!;L P 9
11.03 L S 9,3;G 15.5
*

L G 10
*
*W
C-FOCAL.J4.CODASIII  33534W

01.01 C FSTR USE BY FILES 3,4&9.  SHJ  FILE 10.  SHJ  1 AUG 1979
*
```

```
 101.66
*L G 3
*G
NO. OF CALCS. TO ENTER= 3
ENTER AL,R,L,TC,TH,RI,
:50 :0.015 :0.0833 :510 :560 :1
:100 :0.015 :0.0833 :510 :560 :1
:150 :0.015 :0.0833 :510 :560 :1
```

CASE NO.= 1

AL= 50.0000
CA= 0.015000 L= 0.083300 RO= 0.622912
TC= 510 TH= 560 RI= 1 N= 50 M=
TIME,HR= 0.48
XS= 0.978 BETA= 1.093

Z= 0.4822567992E-002 TIME,HR= 4.65
Z= 0.7410286599E-003 TIME,HR= 4.56
Z= 0.2267622622E-003 TIME,HR= 5.12
Z= 0.8216779679E-004 TIME,HR= 5.35
A= 0.3725233118E-001

I	F2	F2-FL	TCALC	TCALC-TLIN
0	0.910714	0.000000	510.000	0.000
1	0.913289	0.000795	511.441	0.441
2	0.915717	0.001431	512.801	0.801
3	0.918014	0.001943	514.089	1.088
4	0.920202	0.002344	515.313	1.313
5	0.922297	0.002654	516.486	1.486
6	0.924315	0.002887	517.617	1.617
7	0.926260	0.003055	518.711	1.711
8	0.928178	0.003178	519.775	1.775
9	0.930024	0.003238	520.814	1.814
10	0.931848	0.003269	521.838	1.838
11	0.933623	0.003266	522.842	1.842
12	0.935378	0.003235	523.842	1.842
13	0.937109	0.003180	524.841	1.841
14	0.938819	0.003104	525.838	1.838
15	0.940509	0.003009	526.835	1.835
16	0.942195	0.002899	527.833	1.833
17	0.943846	0.002774	528.834	1.834
18	0.945494	0.002637	529.837	1.837
19	0.947130	0.002490	530.844	1.844
20	0.948759	0.002330	531.855	1.855
21	0.950377	0.002163	532.871	1.871
22	0.951973	0.001993	533.893	1.893
23	0.953591	0.001805	534.911	1.911
24	0.955187	0.001618	535.965	1.965
25	0.956778	0.001421	536.996	1.996
26	0.958364	0.001221	538.034	2.034
27	0.959945	0.001016	539.069	2.069
28	0.961522	0.000807	540.102	2.102
29	0.963096	0.000596	541.134	2.134
30	0.964667	0.000382	542.166	2.166
31	0.966238	0.000166	543.203	2.203
32	0.967807	0.000052	544.242	2.242
33	0.969377	0.000265	545.281	2.281
34	0.970950	0.000479	546.322	2.322
35	0.972525	0.000689	547.364	2.364
36	0.974106	0.000894	548.403	2.403
37	0.975694	0.001092	549.436	2.436
38	0.977292	0.001279	550.453	2.453
39	0.978904	0.001453	551.436	2.436
40	0.980533	0.001618	552.406	2.406
41	0.982185	0.001744	553.424	2.424
42	0.983866	0.001941	554.765	2.765
43	0.985584	0.002116	556.127	3.127
44	0.987340	0.002137	557.715	3.715
45	0.989173	0.002493	559.237	4.063
46	0.991074	0.002783	560.681	4.707
47	0.993071	0.003571	562.120	5.538
48	0.995194	0.003935	563.704	6.621
49	0.997488	0.004734	565.517	8.411
50	1.000000	0.000000	566.000	0.000

A= 0.1516477065E-010 C= 0.2257174042E-002 X ERR= 0.007685

CASE NO.= 2

AL= 100.0000
CA= 0.015000 L= 0.083300 RO= 1.245823
TC= 510 TH= 560 RI= 1 N= 78 M=
TIME,HR= 5.43
XS= 0.991 BETA= 1.047

Z= 0.2062842811E-002 TIME,HR= 5.89
Z= 0.4764655685E-003 TIME,HR= 6.33
Z= 0.1533819822E-003 TIME,HR= 6.77
Z= 0.5674979184E-004 TIME,HR= 7.21
A= 0.5294541155E-001

I	F2	F2-FL	TCALC	TCALC-TLIN
0	0.910714	0.000000	510.000	0.000
1	0.912319	0.000329	510.899	0.184
2	0.913883	0.000619	511.775	0.346
3	0.915397	0.000856	512.622	0.468
4	0.916868	0.001052	513.446	0.569
5	0.918303	0.001211	514.250	0.678
6	0.919707	0.001348	515.036	0.758
7	0.921087	0.001444	515.809	0.809
8	0.922446	0.001528	516.576	0.854
9	0.923798	0.001594	517.321	0.893
10	0.925115	0.001646	518.065	0.922
11	0.926430	0.001695	518.801	0.944
12	0.927735	0.001715	519.532	0.960
13	0.929031	0.001735	520.257	0.972
14	0.930319	0.001747	520.979	0.979
15	0.931600	0.001753	521.696	0.982
16	0.932875	0.001753	522.410	0.982
17	0.934145	0.001747	523.121	0.974
18	0.935410	0.001737	523.830	0.973
19	0.936671	0.001722	524.536	0.964
20	0.937928	0.001703	525.240	0.954
21	0.939181	0.001681	525.941	0.941
22	0.940431	0.001655	526.641	0.927
23	0.941677	0.001626	527.339	0.918
24	0.942922	0.001594	528.035	0.892
25	0.944166	0.001551	528.730	0.873
26	0.945398	0.001508	529.423	0.851
27	0.946633	0.001454	530.114	0.820
28	0.947865	0.001436	530.804	0.804
29	0.949094	0.001398	531.492	0.770
30	0.950321	0.001362	532.180	0.751
31	0.951546	0.001291	532.866	0.723
32	0.952768	0.001237	533.550	0.693
33	0.953988	0.001182	534.233	0.662
34	0.955205	0.001124	534.915	0.629
35	0.956421	0.001064	535.596	0.596
36	0.957634	0.001001	536.275	0.561
37	0.958845	0.000936	536.953	0.524
38	0.960053	0.000870	537.630	0.487
39	0.961260	0.000801	538.306	0.448
40	0.962464	0.000730	538.980	0.409
41	0.963667	0.000657	539.653	0.368
42	0.964867	0.000582	540.326	0.326
43	0.966066	0.000505	540.997	0.283
44	0.967263	0.000426	541.667	0.239
45	0.968458	0.000346	542.337	0.194
46	0.969652	0.000264	543.005	0.148
47	0.970843	0.000180	543.672	0.101
48	0.972034	0.000095	544.339	0.053
49	0.973223	0.000009	545.005	0.005
50	0.974412	0.000074	545.671	0.044
51	0.975599	0.000160	546.336	0.093
52	0.976717	0.000254	547.000	0.142
53	0.977974	0.000343	547.665	0.192
54	0.979161	0.000431	548.330	0.241
55	0.980349	0.000518	548.996	0.298
56	0.981548	0.000603	549.662	0.338
57	0.982732	0.000690	550.330	0.384
58	0.983926	0.000765	551.000	0.428
59	0.985138	0.000839	551.675	0.470
60	0.986339	0.000906	552.356	0.507
61	0.987557	0.000963	553.052	0.539
62	0.988717	0.001007	553.751	0.565
63	0.989934	0.001034	554.447	0.581
64	0.991142	0.001045	555.137	0.595
65	0.992357	0.001035	555.834	0.584
66	0.993578	0.000961	556.531	0.542
67	0.994814	0.000850	557.235	0.483
68	0.996060	0.000697	557.945	0.400
69	0.997381	0.000493	558.640	0.297
70	1.000000	0.000000	560.000	0.000

A= 0.2939173466E-009 C= 0.1062365844E-002 X ERR= 0.027612

CASE NO.= 3

AL= 150.0000
CA= 0.015000 L= 0.083300 RO= 1.868735
TC= 510 TH= 560 RI= 1 N= 185 M=
TIME,HR= 7.33
XS= 0.995 BETA= 1.031

Z= 0.1261275378E-002 TIME,HR= 6.32
Z= 0.3667662483E-003 TIME,HR= 9.25
Z= 0.1187762981E-003 TIME,HR= 10.24
Z= 0.4386359815E-004 TIME,HR= 11.28
A= 0.5327182768E-001

I	F2	F2-FL	TCALC	TCALC-TLIN
0	0.910714	0.000000	510.000	0.000
1	0.911716	0.000152	510.561	0.085
2	0.912711	0.000296	511.118	0.166
3	0.913687	0.000421	511.664	0.236
4	0.914665	0.000529	512.281	0.296
5	0.915588	0.000622	512.729	0.348
6	0.916517	0.000701	513.248	0.393
7	0.917436	0.000769	513.764	0.431
8	0.918345	0.000828	514.273	0.464
9	0.919247	0.000879	514.776	0.492
10	0.920141	0.000924	515.279	0.517
11	0.921038	0.000962	515.777	0.539
12	0.921914	0.000996	516.272	0.558
13	0.922794	0.001025	516.765	0.574
14	0.923670	0.001051	517.255	0.589
15	0.924543	0.001074	517.744	0.601
16	0.925413	0.001093	518.231	0.612
17	0.926280	0.001110	518.717	0.622
18	0.927146	0.001125	519.202	0.630
19	0.928009	0.001138	519.685	0.637
20	0.928870	0.001149	520.169	0.643
21	0.929727	0.001158	520.652	0.648
22	0.930581	0.001163	521.129	0.650
23	0.931444	0.001172	521.609	0.656
24	0.932299	0.001177	522.088	0.659
25	0.933153	0.001181	522.566	0.661
26	0.934006	0.001183	523.044	0.663
27	0.934858	0.001185	523.521	0.663
28	0.935708	0.001185	523.997	0.663
29	0.936556	0.001184	524.473	0.663
30	0.937407	0.001182	524.948	0.662
31	0.938254	0.001180	525.422	0.661
32	0.939101	0.001176	525.896	0.658
33	0.939946	0.001171	526.370	0.656
34	0.940791	0.001165	526.843	0.653
35	0.941635	0.001159	527.316	0.649
36	0.942478	0.001151	527.787	0.645
37	0.943320	0.001143	528.259	0.640
38	0.944161	0.001133	528.730	0.635
39	0.945001	0.001123	529.200	0.629
40	0.945840	0.001112	529.670	0.623
41	0.946678	0.001100	530.140	0.616
42	0.947516	0.001087	530.609	0.609
43	0.948352	0.001073	531.077	0.601
44	0.949188	0.001059	531.545	0.593
45	0.950022	0.001044	532.013	0.584
46	0.950857	0.001027	532.480	0.575
47	0.951690	0.001010	532.947	0.566
48	0.952523	0.000992	533.413	0.556
49	0.953354	0.000973	533.878	0.545
50	0.954185	0.000954	534.344	0.534
51	0.955015	0.000933	534.809	0.523
52	0.955844	0.000912	535.273	0.511
53	0.956672	0.000890	535.736	0.498
54	0.957500	0.000867	536.200	0.485
55	0.958326	0.000843	536.663	0.472
56	0.959152	0.000819	537.125	0.458
57	0.959977	0.000793	537.587	0.444
58	0.960801	0.000767	538.048	0.429
59	0.961624	0.000740	538.510	0.414
60	0.962447	0.000712	538.970	0.399
61	0.963268	0.000683	539.430	0.383
62	0.964089	0.000654	539.890	0.366
63	0.964909	0.000623	540.349	0.349
64	0.965725	0.000592	540.809	0.332
65	0.966547	0.000561	541.266	0.314
66	0.967365	0.000529	541.724	0.296
67	0.968181	0.000494	542.182	0.277
68	0.968998	0.000460	542.639	0.258
69	0.969813	0.000425	543.095	0.238
70	0.970629	0.000390	543.551	0.218
71	0.971441	0.000353	544.007	0.198
72	0.972255	0.000316	544.463	0.177
73	0.973067	0.000278	544.919	0.156
74	0.973879	0.000239	545.372	0.134
75	0.974692	0.000200	545.828	0.112
76	0.975508	0.000160	546.280	0.090
77	0.976310	0.000120	546.734	0.067
78	0.977119	0.000079	547.187	0.044
79	0.977928	0.000037	547.640	0.021
80	0.978736	0.000005	548.092	0.003
81	0.979544	0.000044	548.545	0.025
82	0.980351	0.000091	548.997	0.051
83	0.981158	0.000134	549.449	0.075
84	0.981965	0.000178	549.901	0.099
85	0.982773	0.000221	550.353	0.123
86	0.983580	0.000264	550.805	0.148
87	0.984387	0.000307	551.257	0.172
88	0.985195	0.000350	551.709	0.196
89	0.986004	0.000391	552.162	0.219
90	0.986813	0.000432	552.615	0.242
91	0.987622	0.000471	553.070	0.263
92	0.988430	0.000507	553.525	0.284
93	0.989254	0.000541	553.982	0.303
94	0.990074	0.000572	554.445	0.320
95	0.990890	0.000593	554.903	0.335
96	0.991729	0.000610	555.369	0.346
97	0.992564	0.000621	555.837	0.354
98	0.993413	0.000625	556.311	0.356
99	0.994271	0.000627	556.792	0.351
100	0.995145	0.000623	557.281	0.338
101	0.996039	0.000568	557.782	0.314
102	0.996955	0.000491	558.296	0.275
103	0.997911	0.000389	558.830	0.217
104	0.998913	0.000236	559.391	0.132
105	1.000000	0.000000	560.000	0.000

A= 0.7140756094E-009 C= 0.1425975095E-002 X ERR= 0.023757

Focal Program Nomenclature for Program in Appendix B

Symbol	Definition
A	Trapezoidal area
AL	α
L	Batt thickness
N	Number of increments
Q	Heat flow rate
CA	k
TH	τ_H
TC	τ_c
SI	σ = 0.1714 E-8
KEFF	k_{eff}
T2	New reduced temperature distribution
T1	Old reduced temperature distribution
TL, DF, T3, T4	Output convenience variables
NK, J, IV, I, KK, KA, JJ, M IN, K	Indices
D1, EG, DU, D2, EF	Convenience Variables
RI	Refractive index
NO	Number of cases
RC	Defined in line 15.32 File 3
W1	Defined in 01.32 File 4
BE	b
XS	Defined in 01.34 File 4
D	Defined in 03.10 File 4
G, G1	Defined in Group 4 File 4
E1, E2E3, E4	$E_1(x)$, $E_2(x)$, $E_3(x)$, $E_4(x)$ integrals
AQ, A1, A2, A3, A4, A5, B1, B2, B3, B4, C1, C2, C3, C4	Parameters set in Group 14 of File 4
EI	$E_1(-x)$
Z	Error defined in Group 10 File 9
U	Old value of EF

THIS PAGE

WAS INTENTIONALLY

LEFT BLANK

APPENDIX C

PDP/8e FOCAL PROGRAM LISTING, TYPICAL OUTPUT, AND NOMENCLATURE LIST FOR THREE-REGION APPROXIMATION

```
C- FOCAL.J4.CODASIII  33534W

01.01 C THREE REGION RAD/COND. FILE 85 SHJ 20 MARCH 80
01.02 C INPUT IS IN BTU, HR, FT, DEG. R UNITS.
01.03 C OUTPUT IS IN BTU, IN, HR, FT, DEG. R UNITS
01.05 A "PR, EP, N0 ?" PR, EP, N0; T !; S N=0; T "AL, XL, CA, TH, TC, EH, EC ?"
01.06 S N=N+1
01.10 A AL(N), XL(N), CA(N), TH(N), TC(N), EH(N), EC(N); T !
01.11 I (N-N0)1.06; S N=0
01.12 S N=N+1; S AL=AL(N); S XL=XL(N); S CA=CA(N); S TH=TH(N); S TC=TC(N)
01.13 S EH=EH(N); S EC=EC(N)
01.15 S I=0; S SI=.1714E-8; S T1(1)=TH; S T2(1)=TC
01.20 S R1=1/(CA*AL/PR+SI*EH*(TH↑2+T1(1)↑2)*(TH+T1(1)))
01.25 S R2=(XL*AL-2*PR)/(CA*AL+(4/3)*SI*(T1(1)↑2+T2(1)↑2)*(T1(1)+T2(1)))
01.30 S R3=1/(CA*AL/PR+SI*EC*(T2(1)↑2+TC↑2)*(T2(1)+TC))
01.35 S I=I+1
01.40 S T1=TH+(TC-TH)*R1/(R1+R2+R3)
01.45 S T2=TC+(TH-TC)*R3/(R1+R2+R3)
01.50 I (-FABS((T1-T1(1))/T1(1))+EP)1.6,1.6
01.55 I (FABS((T2-T2(1))/T2(1))-EP)1.7
01.60 S T1(1)=T1; S T2(1)=T2; I (I-100)1.2
01.65 GOTO 2.05
01.70 S Q=(TH-TC)/(R1+R2+R3)
01.75 S CP=12*Q*XL/(TH-TC)
01.90 T "CA=", %11.04, CA, "  AL=", AL, "  XL=", XL, "  EH=", EH, !
01.91 T "EC=", EC, "  TH=", TH, "  TC=", TC, "  PR=", PR, !
01.92 T "EP=", EP, !
01.95 T "Q=", %11.06, Q, "  CP=", CP, !
01.96 T "T1=", T1, "  T2=", T2, !

02.01 I (N-N0)1.12; Q
02.05 D 1.9; D 1.91; D 1.92; T "**** DID NOT CONVERGE ****", !
02.10 I (N-N0)1.12; Q
*
```

```
 L G 85
*G
PR, EP, NO ?: 0.69315 : 1E-4 : 3
AL, XL, CA, TH, TC, EH, EC ?: 50 : 0.0833 : 0.015 : 560 : 510 : 1 : 1
: 100 : 0.0833 : 0.015 : 560 : 510 : 1 : 1
: 150 : 0.0833 : 0.015 : 560 : 510 : 1 : 1
CA=        0.0150   AL=       50.0000   XL=        0.0833   EH=        1.0000
EC=        1.0000   TH=      560.0000   TC=      510.0000   PR=        0.6932
EP=        0.0001
Q=      22.447040   CP=       0.448761
T1=    550.042566   T2=     521.103533
CA=        0.0150   AL=      100.0000   XL=        0.0833   EH=        1.0000
EC=        1.0000   TH=      560.0000   TC=      510.0000   PR=        0.6932
EP=        0.0001
Q=      16.591717   CP=       0.331702
T1=    555.050597   T2=     515.372918
CA=        0.0150   AL=      150.0000   XL=        0.0833   EH=        1.0000
EC=        1.0000   TH=      560.0000   TC=      510.0000   PR=        0.6932
EP=        0.0001
Q=      14.259955   CP=       0.285085
T1=    556.788139   T2=     513.423984
*
```

Nomenclature for Program in Appendix C.

Symbol	Identification
CP	Apparent thermal conductivity
EC	Constants set equal to 1
EH	Constants set equal to 1
EP	Convergence criteria, 1×10^{-4}
NO	Number of data sets < 100
PR	Dimensionless boundary region thickness, 0.69315
R1	Thermal resistance of region I
R2	Thermal resistance of region II
R3	Thermal resistance of region III
T1	Absolute temperature at interface I/II
T2	Absolute temperature at interface II/III

APPENDIX D

FORTRAN PROGRAM FOR THREE-REGION APPROXIMATION

The following program outputs values for the temperature at the interior points which divide the total insulation thickness into three regions. The temperature calculations include an output for the temperature profile in the middle region.

Identification of Variables

XK — thermal conductivity of air
XL — specimen thickness
TC — temperature of cold boundary
TG — temperature of hot boundary
T1 — temperature between regions 2 and 3
T2 — temperature between regions 1 and 2
Q — heat flux
CP — effective thermal conductivity of specimen
AL — alpha, defined in nomenclature
RI — refractive index
FR — parameter defining thickness of regions 1 and 3
EP — convergence criterion
SI — Stefan-Boltzmann constant
EH — emissivity of cold plate
EC — emissivity of hot plate
X — distance into specimen

Program Listing

```
 P1CC:3911
C0100            DIMENSION XK(7),XL(7),TC(7),T1(7,7,7),T2(7,7,7),TG(7),
C0200           1Q(7,7,7),CP(7,7,7),X(20),T(20)
C0300            DATA XK/.013207,.014178,.014834,.015,.015115,.015795,.01
6670/
C0400            DATA XL/.0333,.25,5*0.0/
00500            DATA TC/435.0,475.0,505.0,510.0,515.0,545.0,585.0/
C0600            AL=200.
00700            DATA TG/485.,525.,555.,560.,565.,595.,635./
C0800            RI=1.0
00900            FR=.69315
C1000            EP=.00001
C1100            SI=.1714E-8
01200            EH=1.
01300            EC=1.
01400            DO 100 I=1,7
01500            DO 100 J=1,2
01600            K=I
C1605            TH=TG(I)
C1610            T1A=TC(K)
C1620            T2A=TH
C1630            NC=0
C1700    17      NC=NC+1
C1800            IF ( NC.GT.100) GO TO 99
02100            R1=1./(XK(I)*AL/FR+SI*EH*(T1**2+T1A**2)*(TH+T1A))
C2200            R2=(XL(J)*AL-2*FR)/(XK(I)*AL+(1.3333)*SI*(T1A**2
C2300           1+T2A**2)*(T1A+T2A))
02400            R3=1./(XK(I)*AL/FR+SI*EC*(T2A**2+TC(K)**2)*(T2A+TC(K)))
C2500            T1B=TH+(TC(K)-TH)*R1/(R1+R2+R3)
02600            T2B=TC(K)+(TH-TC(K))*R3/(R1+R2+R3)
02700            TST1=ABS((T1B-T1A)/T1A)
02800            TST2=ABS((T2B-T2A)/T2A)
02900            IF (TST1.LT.EP.AND.TST2.LT.EP) GO TO 95
C2910            T1A=T1B
C292C            T2A=T2B
C3000            GO TO 17
C3100    95      T1(I,J,K)=T1B
C3200            T2(I,J,K)=T2B
C3300            GO TO 96
C3400    99      TYPE 1000,I,J,K
C3500    1000    FORMAT(2X,' NO CONV.',3I3)
C3600
C3700    96      Q(I,J,K)=(TH-TC(K))/(R1+R2+R3)
C3800            CP(I,J,K)=12.*Q(I,J,K)*XL(J)/(TH-TC(K))
C3900    100     CONTINUE
C3905            TYPE 150
C3910    150     FORMAT(3X,'INDEX',3X,'K',3X,'LENGTH',3X,'T COLD',3X,
C3911          1' T* ',3X,' T* ',3X,'T HOT',4X,' Q ',5X,'X EFF')
*
```

```
 P4CCC:8100
C4000             DØ 200 I=1,7
C4100             DØ 200 J=1,2
C4200             K=I
C4300             TYPE 1001,I,J,K,XK(I),XL(J),TC(K),T2(I,J,K)
C4301            1 ,T1(I,J,K),TG(K),Q(I,J,K),CP(I,J,K)
C4400    1001     FØRMAT(1X,3I2,F9.6,F7.4,4F3.2,2F8.4)
C4500    200      CØNTINUE
C4600             TYPE 1002,(XK(I),I=1,4)
C4700             TYPE 1002,(XL(J),J=1,7)
C4800             TYPE 1002,(TC(K),K=1,6)
C4900    1002     FØRMAT(2X,7F9.3)
C5100             DØ 400 I=1,7
C5200             DØ 400 J=1,2


PAGE 2
C5300             K=I
C5400             T(1)=T2(I,J,K)
C5500             DØ 395 L=2,11
C5600             X(1)=FR/AL
C5700             DX=(XL(J)-2*X(1))/10.0
C5800             X(L)=X(1)+(L-1)*DX
C5900             TP=T(L-1)
C6000             A=(4*SI)/(3*AL)
C6100             B=XK(I)
C6200             NC=1.
C6300    30       C=(Q(I,J,K))*((L-1)*DX)+XK(I)*T2(I,J,K)+A*T2(
C6400           1 I,J,K)**4
C6500
C6600             NC=NC+1
C6700             IF (NC.GT.100) GØ TØ 215
C6800             CF=(A*TP**4+B*TP-C)/(4*A*TP**3+B)
C6900             IF ( ABS(CF).LT.EP) GØ TØ 21
C7000             TP=TP-CF
C7100             GØ TØ 30
C7200    21       T(L)=TP
C7300    395      CØNTINUE
C7400             TYPE 1003,        I,J,K
C7500    1003     FØRMAT(2X,3I3)
C7510             TYPE 160
C7520    160      FØRMAT(1X,'X VALUE    TEMP')
C7600             DØ 398 L=1,11
C7700             TYPE 1004,X(L),T(L)
C7800    1004     FØRMAT(2X,F8.6,F10.3)
C7900    398      CØNTINUE
C8000    400      CØNTINUE
C8010    215      TYPE 1005,L
C8020    1005     FØRMAT(2X,' T DID NØT CØNVERGE',I3)
C8025             GØ TØ 400
C8100             END
*
```

Sample Output for $\alpha = 200$

INDEX	K	LENGTH	T COLD	T*	T*	T HOT	Q	K EFF
1 1 1	0.013207	0.0333	435.00	437.39	432.71	435.00	10.4351	0.2096
1 2 1	0.013207	0.2500	435.00	435.30	434.23	435.00	3.5203	0.2112
2 1 2	0.014178	0.0333	475.00	477.44	522.68	525.00	11.7907	0.2357
2 2 2	0.014173	0.2500	475.00	475.32	524.22	525.00	3.9635	0.2373
3 1 3	0.014834	0.0333	505.00	507.48	552.65	555.00	12.8375	0.2566
3 2 3	0.014834	0.2500	505.00	505.33	554.21	555.00	4.3194	0.2592
4 1 4	0.015000	0.0333	510.00	512.48	557.64	560.00	13.0181	0.2603
4 2 4	0.015000	0.2500	510.00	510.34	559.21	560.00	4.3309	0.2629
5 1 5	0.015115	0.0333	515.00	517.49	562.64	565.00	13.2001	0.2639
5 2 5	0.015115	0.2500	515.00	515.34	564.21	565.00	4.4429	0.2666
6 1 6	0.015795	0.0333	545.00	547.53	592.61	595.00	14.3309	0.2365
6 2 6	0.015795	0.2500	545.00	545.35	594.20	595.00	4.3231	0.2397
7 1 7	0.016670	0.0833	585.00	587.58	632.57	635.00	15.9437	0.3137
7 2 7	0.016670	0.2500	585.00	585.87	634.18	635.00	5.3786	0.3227

1 1 1

X VALUE	TEMP
.003466	437.394
.011103	442.078
.018739	446.729
.026376	451.345
.034013	455.927
.041650	460.476
.049287	464.991
.056924	469.472
.064561	473.919
.072197	478.333
.079834	482.714

1 2 1

X VALUE	TEMP
.003466	435.804
.027773	440.821
.052079	445.799
.076386	450.738
.100693	455.639
.125000	460.500
.149307	465.324
.173614	470.108
.197921	474.855
.222227	479.563
.246534	484.233

ORNL/TM-7481
Distribution
Category UC-95d

INTERNAL DISTRIBUTION

1–2.	Central Research Library	190–199.	S. H. Jury
3.	Document Reference Section	200.	H. M. Long
4–5.	Laboratory Records	201–210.	T. S. Lundy
6.	Laboratory Records, ORNL RC	211–220.	D. L. McElroy
7.	Patent Office	221.	A. E. Pasto
8–167.	M&C Division Office	222.	T. F. Scanlan
168.	A. J. Caputo	223–227.	A. C. Schaffhauser
169.	R. S. Carlsmith	228.	J. O. Stiegler
170.	P. T. Carlson	229.	V. J. Tennery
171.	J. A. Carpenter, Jr.	230–239.	D. W. Yarbrough
172.	E. A. Creswick	240.	A. L. Bement, Jr. (Consultant)
173.	D. P. Edmonds	241.	E. H. Kottcamp, Jr. (Consultant)
174–183.	H. A. Fine	242.	Alan Lawley (Consultant)
184.	T. G. Godfrey, Jr.	243.	T. B. Massalski (Consultant)
185–187.	M. R. Hill	244.	M. J. Mayfield (Consultant)
188.	H. W. Hoffman	245.	R. H. Redwine (Consultant)
189.	R. R. Judkins	246.	John Stringer (Consultant)

EXTERNAL DISTRIBUTION

247. P. R. Achenbach, 1322 Kurtz Road, McLean, VA 22101

248. R. W. Anderson, Energy Consultant, 7090 Tecomsen Lane, Chanhassen, MN 55317

249. BABCOCK & WILCOX COMPANY, Alliance Research Center, 1562 Beeson Street, Alliance, OH 44601

H. W. Wahle

250. C E A INC., 61 Taylor-Reed Place, Stamford, CT 06096

F. A. Govan

251. CERTAIN-TEED PRODS. CORP., P.O. Box 860, Valley Forge, PA 19482

J. F. Kimpflen

252. CERTAINTEED CORP., 1400 Union Meeting Rd., Blue Bell, PA 19422

D. J. McCaa

253. DOW CHEMICAL COMPANY, Granville Research Center, P.O. Box 515, Granville, OH 43023

D. Greason

254. FEDERAL TRADE COMMISSION, 414 11th Street, Star Building, Washington, DC 20580

K. C. Howerton

255. FIBER MATERIALS, Biddeford Industrial Park, Biddeford, ME 04005

R. P. Tye

256. GENERAL SERVICES ADMINISTRATION, 18 and F Streets, NW, Washington, DC 20405

C. L. Carter

257. GEOSCIENCE LTD., 410 S. Cedros Ave., Solana Beach, CA 92075

H. F. Poppendick

258. Charles Gilbo, 201 E. Ross Street, Lancaster, PA 17602

259. W. R. GRACE & CO., 62 Wittemore Ave., Cambridge, MA 02140

J. W. Howanski

260. HAUSER LABORATORIES, 5680 Central Ave., P.O. Box G, Boulder, CO 80302

R. L. Hauser

261. INSTITUTO DI FISICA TECHNICA, FACOLTA INGEGNERIA-UNIV PADOVA, Via F Marzolo N9, Padova 35100 Italy

F. DePonte

262. JOHNS-MANVILLE RESEARCH AND DEVELOPMENT CENTER, P.O. Box 5108, Denver, CO 80217

C. M. Pelanne

263. LAWRENCE BERKELEY LABORATORY, University of California, Bldg. 90, Rm. 3058, Berkley, CA 94720

W. L. Carroll

264. LOUISIANA PACIFIC CORP., PABCO INSULATION DIV., 1110 16 RD., Fruita, CO 81521

F. B. Hutto, Jr.

265. C. F. Lucks, 1858 W. Lane Ave., Columbus, OH 43221

266. MINERAL INSULATION MANUFACTURERS ASSOCIATION, 382 Springfield Ave., Summit, NJ 07901

S. Cady

267. NATIONAL ASSOCIATION OF HOME BUILDERS, RESEARCH FOUNDATION, INC., 627 Southlawn Lane, Rockville, MD 20850

H. D. Angelton

268–272. NATIONAL BUREAU OF STANDARDS, DEPARTMENT OF COMMERCE, Gaithersburg, Washington, DC 20234

R. Dils
F. J. Powell
B. Peavy
B. G. Rennex
M.C.I. Siu

273. NATIONAL BUREAU OF STANDARDS-BOULDER, CYROGENICS DIVISION, INSTITUTE FOR BASIC STANDARDS, Boulder, CO 80303

J. G. Hust

274–275. NATIONAL RESEARCH COUNCIL OF CANADA, Montreal Road, Ottawa Ontario K1A OR6, Canada

M. Bomberg
C. J. Shirtliffe

276. OWENS-CORNING FIBERGLASS CORP., Technical Center, Box 415, Granville, OH 43023

M. Hollingsworth, Jr.

277. PITTSBURGH CORNING CORP., 800 Presque Isle Drive, Pittsburgh, PA 15239

R. W. Gerrish

278. ROCKWOOL INDUSTRIES, INC., P.O. Box 5170, Denver, CO 80217

S. L. Matthews

279. ROCKWOOL INDUSTRIES, INC., Leeds, AL 35094

E. F. Cusick, Jr.

280. ST. GOBAIN ISOVER, CENTRE DE RECHERCHES INDUSTRIELLE DE RANTIGNY, 60290 Rantigny, France

Catherine Langlais

281. STATE UNIVERSITY OF NEW YORK-STONY BROOK, Engineering Department, Stony Brook, NY 11794

A. L. Berlad

282. W. C. Turner, 713 Forest Circle, South Charles, WV 25303

283. JIM WALTER RESEARCH CORP., 10301 9th Street, North, St. Peterburg, FL 33702

G. Miller

284–289. DOE CONSERVATION AND SOLAR ENERGY, The Forestal Bldg., 1000 Independence Ave., Washington, DC 20585

M. Savitz, Deputy Assistant Secretary

Office of Buildings and Community Systems

E. C. Freeman, Program Manager, Architectural and Engineering Branch

E. L. Bales
John Cable
J. P. Millhone

Office of Industrial Programs

M. McNeil

290. DOE OAK RIDGE OPERATIONS OFFICE, P.O. Box E, Oak Ridge, TN 37830

Office of Assistant Manager for Energy Research and Development Office

291–562. DOE, TECHNICAL INFORMATION CENTER, OFFICE OF INFORMATION SERVICES, P.O. Box 62, Oak Ridge, TN 37830

For distribution as shown in TID-4500 Distribution Category, UC-95d (Energy Conservation — Buildings and Community Systems)

☆ U.S. GOVERNMENT PRINTING OFFICE: 1980-740-062/369